Fig. 6. Ultrastructural localization of drebrin A in postnatal day (PNd) 7 cortex. Horseradish peroxidase–diaminobenzidine was used to detect the presence of drebrin A. **A:** A large-caliber axon that is largely devoid of vesicles, yet synaptically associated with two dendritic processes. Of the two small clusters of vesicles, only one is at a synapse. The synapse showing a slight indentation of the plasma membrane, perhaps an early sign of spine neck formation, lacks vesicles presynaptically. Both synapses show accumulation of drebrin A immunoreactivity along the postsynaptic membrane (arrows). **B:** A dendrite lacking morphologically identifiable synapses. Drebrin A immunoreactivity has accumulated along small protrusions (asterisks). **C:** A well-established spine head forming a synapse with an axon. The axon contains a moderate number of vesicles that are clustered at the synaptic junction, and the postsynaptic membrane (arrow) is slightly immunoreactive. Drebrin A immunoreactivity is more intense along the nonsynaptic portions of the plasma membrane. The nonsynaptic portions of the dendrite contain no detectable microtubules and also exhibit plasma membranes with irregular contours. **D:** A dendrite containing well-defined microtubules. Drebrin A immunoreactivity is evident along a slight protruding portion of the shaft (synapse 1) and along a spine with narrow neck (synapse 2) but whose presumably "presynaptic" profile shows no vesicle clustering near the juxtaposed portion of membrane. Drebrin A immunoreactivity is also associated with a dendritic shaft forming an asymmetric synapse (synapse 3) opposite of another protuberance (asterisk) and another dendritic protuberance (synapse 4) whose presynaptic element shows adult-like vesicle clustering. **E:** A dendrite bearing a spine that stains strongly for drebrin A. The neurite with which this immunoreactive spine is associated shows only a few vesicles, scattered widely and away from the juxtaposed portion of the plasma membrane. In contrast, the other presynaptic element associated with an unlabeled spine (arrowhead) of the same dendrite contains a large cluster of vesicles. Scale bar = 500 nm in E (applies to B–E); 650 nm for A.

TABLE 3. Ultrastructural Characteristics of Synapses in Relation to Drebin A: PNd7 Cortex (149 Encountered Synapses)

Asymmetric 93				Symmetric 56			
Labeled 40		Unlabeled 53		Labeled 18		Unlabeled 38	
Mature 2	Immature 38	Mature 4	Immature 49	Mature 0	Immature 18	Mature 0	Immature 38

PNd, postnatal day.

PSDs were often absent (left arrow in Fig. 6A, Fig. 6C) and the putatively presynaptic profile contained either no vesicle near the junctional membrane (Fig. 6A,D), only a few vesicles (right synapse with straight arrow in Fig. 6A, synapse 1 of Fig. 6D, Fig. 6E), or many more vesicles that were removed from the junctional membrane (synapse 2 in Fig. 6D). We noted that some dendritic profiles showed more intense drebrin A immunoreactivity in the nonjunctional portions than in the synaptic portions (e.g., Fig. 6C).

Majority of asymmetric synapses are immature and unlabeled for drebrin A. Quantitative analysis was performed upon neonatal cortex, categorizing synapses either as newly formed, immature, and presumed to be synaptic, or as mature. The number of vesicles, detectability of PSDs and narrowness of spine necks were used as criteria to distinguish between the two categories. Those intercellular contact sites lacking both the PSDs and vesicles were categorized as nonsynaptic. Twenty-six nonoverlapping fields were surveyed from which were found 149 synaptic profiles (labeled and unlabeled, asymmetric and symmetric) and 31 nonsynaptic immunolabeled profiles. Ninety-six percent of these profiles appeared immature, using the above criteria. Unlike the adult tissue, in which the majority of synapses were immunolabeled (114 of 190), only a minority (58 of 149) of the synaptic junctions encountered in PNd7 cortex were drebrin A immunoreactive (Labeled, symmetric + asymmetric; Table 3). This difference across the ages was statistically significant (58 ± 4% for adults, 31 ± 4% for PNd7 tissue; $P < 0.0005$, two-tailed unpaired t test). Among the synapses identifiable as asymmetric, the majority of those in the PNd7 cortex (53 of 93) were also unlabeled, as opposed to the adult cortex, for which only 36 of the 147 asymmetric synapses were unlabeled (Table 3). This difference across the ages was statistically significant (59 ± 8% for PNd7; 23 ± 5% for adult; $P < 0.005$, two-tailed unpaired t test).

Larger proportion of the presumptive immature symmetric synapses is immunolabeled for drebrin A. Another notable departure from adult tissue was the prevalence of drebrin A at symmetric junctions. Thirty-two percent (18 of 56) of the presumptive immature symmetric synapses in PNd7 cortex were immunolabeled (Table 3). Compared with the adult tissue, many more of the neonatal synapses were classified as symmetric, due to the absence of the PSDs (38% for PNd7-tissue, 23% for adult tissue; Table 3). Most likely, many of these were glutamatergic synapses in which the PSD had not yet assumed their mature thick form and in which the spine necks had not yet narrowed (Aoki et al., 1994; Aoki, 1997).

Two PEG immunolabeling results supported the above presumption that neonatal synapses exhibiting drebrin A are excitatory. One was that the axons identifiable to be presynaptic to the drebrin A-positive dendritic membrane were almost always GABA-negative (more than 90% of the drebrin A-positive synapses encountered, an example shown in Fig. 7), with some of the exceptions consisting of dendrites receiving convergent inputs from multiple axons that included GABA-positive ones. The second was that dendritic membranes, revealed to be drebrin A-positive by the SIG label (detailed below), also were immunopositive for the NR2B subunit of NMDA receptors (an example shown in Fig. 8).

Adult tissue, immunolabeled for drebrin A using SIG, exhibit dendritic localizations. Another set of tissue was immunolabeled using SIG, so as to be able to analyze the distribution of drebrin A within postsynaptic profiles. Although light microscopy indicated only low amounts of drebrin A in perikarya and dendritic trunks, electron microscopy revealed discrete labeling along the intracellular surface of perikarya (data not shown). These immunoreactive sites of perikaryal plasma membranes were not synaptic. The immunoreactive patches of the membrane typically occurred adjacent to arrays of endoplasmic reticulum.

Synaptic labeling with SIG was exclusively postsynaptic and at asymmetric synapses. The proportion of synapses labeled (30 of 51 or 59%) was lower than that seen using HRP-DAB (111 of 147 or 76%), indicating that many more synapses may have expressed drebrin A but at amounts too low to be detectable by the less-sensitive SIG procedure. Nevertheless, the SIG-labeled tissue could be used to reveal more precise information regarding the intracellular distribution of drebrin A. Drebrin A was detected immediately adjacent to PSDs (Fig. 9B). However, more often, SIG particles within dendrites occurred along membranous portions removed from PSDs (Fig. 9A), indicating that a larger pool of drebrin A exists at nonjunctional sites.

Neonatal tissue, labeled using SIG, shows enrichment of drebrin A at presumptive immature synapses. Neonatal tissues were also subjected to drebrin-A immunolabeling using SIG. As expected, the proportion of synaptic profiles labeled by the SIG label was less, compared with the HRP-DAB labeling. Nevertheless, the SIG labeling resembled the DAB labeling's developmental pattern, in that the proportion of synapses labeled was less at PNd7 (9 of 31 or 29%) than in adulthood (59%).

The SIG procedure revealed an additional feature regarding drebrin A, namely that the presumptive immature synapses are more frequently labeled than are the synapses with relatively more established morphological characteristics. Some of the immunoreactive sites showed no intercellular specializations, whereas other immunoreactive sites were synapses with distinctively immature features (arrowheads in Fig. 10). In contrast, mature synapses with clearly identifiable PSDs in the immediate vicinity were frequently unlabeled (open arrows in Fig. 10). Over the scanned area, only 1 of the 24 mature synapses encountered within PNd7 tissue was immunolabeled by SIG, in contrast to 9 of the 21 presumptive immature synapses encountered that were immunolabeled. These observations indicated that the amount of

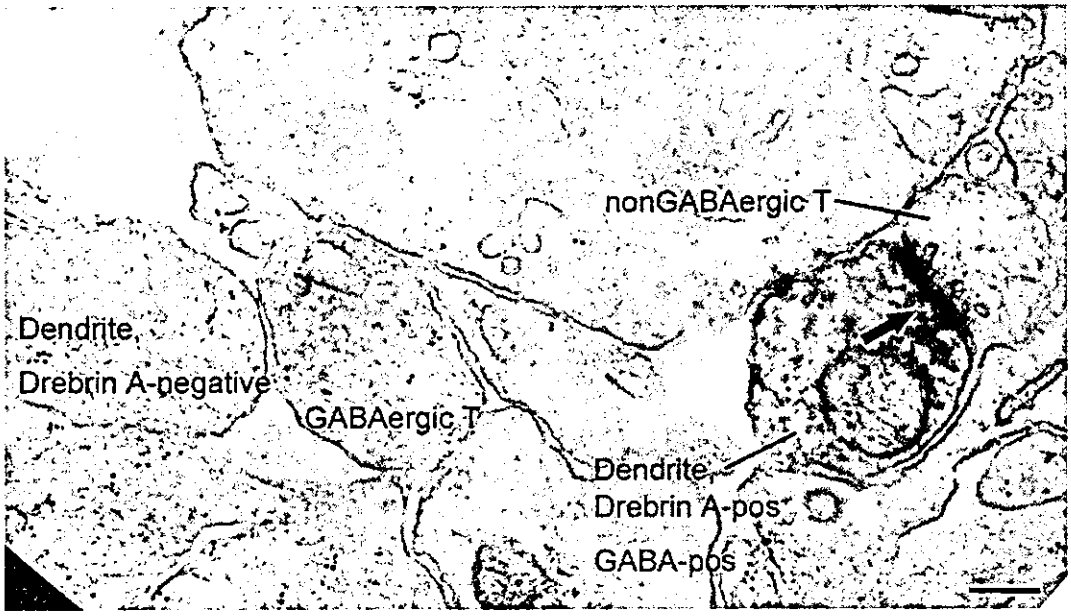

Fig. 7. Drebrin A is postsynaptic to γ-aminobutyric acid (GABA) -negative terminals of postnatal day (PNd) 7 tissue. At PNd7, dendrites rarely exhibit axospinous asymmetric synapses, thereby making the distinction between excitatory and inhibitory synapses more difficult than for adult tissue. The section shown here was dually labeled for drebrin A (by horseradish peroxidase–diaminobenzidine [HRP-DAB]) and for the inhibitory neurotransmitter, GABA by the postembedding gold immunolabeling procedure (PEG). The 10-nm colloidal particles reflect GABA immunoreactivity. GABA immunoreactivity is detectable in one profile that appears to be an axon terminal (GABAergic T), based on the presence of a few vesicles. This profile is juxtaposed to a drebrin A-negative profile that is likely to be a dendrite. In contrast, the dendrite to the right is HRP-DAB–labeled for drebrin A (Drebrin A-pos) and is also immunoreactive for GABA (GABA-pos). However, its presynaptic terminal is completely devoid of 10-nm colloidal gold particles, indicating that is it non-GABAergic (nonGABAergic T). The arrow points to the postsynaptic membrane over which drebrin A accumulates. Scale bar = 200 nm.

drebrin A expressed at single synapses varied, with mature synapses exhibiting relatively less than the newly forming ones. Examples were seen where two axons converged upon a single postsynaptic profile, with each axon abutting a distinct spine head (Fig. 10B). Here, too, drebrin A immunoreactivity was more robust within the less mature spine head, so identified by the absence of PSD and absence of vesicle clusters within the abutting portion of the axon.

Although the SIG labeling for drebrin A was not strictly along the postsynaptic membrane (small arrows in Fig. 10), it appeared to be biased toward the inner surface of the dendritic plasma membrane, rather than being distributed evenly in the cytosol. Quantitative analysis of SIG particle positions showed that the above impressions regarding the membranous bias of labeling were valid. The 331 SIG particles encountered within the 46 nonoverlapping surveyed fields were collected from two PNd7 and two adult brains; 20% of the SIG particles occurred directly on the membrane, and 45% remained within 50 nm from the plasma membrane. This distance corresponded to the 0 to 10% distance from the plasma membrane, relative to the diameter of the profiles (Fig. 11). This proximity of drebrin A sites to the membrane was relatively more prominent for the PNd7 tissue. Specifically, 56% of the SIG particles for one PNd7 tissue occurred within the 10% distance from the plasma membrane, and the corresponding value for the other PNd7 tissue was 64%. Both of these values were greater than the value obtained for the two adult tissue—40% and 41% (Fig. 11). However, data from more animals will need to be collected before we can be certain about the age-dependent differences.

Western blotting reveals developmental loss of drebrin A in the supernatant. The electron microscopic observation showing association of drebrin A with the intracellular surface of the plasma membrane prompted us to further quantify the subcellular distribution of drebrin. To this end, Western blotting was performed to obtain quantitative measures of drebrin in the supernatant (mostly free cytosolic, but also including drebrin associated with the membrane) and in the pellet (mostly associated with F-actin and microsomes) fractions (Fox, 1985; Crosbie et al., 1991). Based on the developmental data obtained from Western blotting (Fig. 2), PNd8 was taken as the representative ages of the neonatal stage (where a large portion of the drebrin is still in the E-isoform), whereas PNd16 was taken as the representative, youngest adult-like stage, in which the A-isoform dominates.

Quantitative analysis of drebrin content in the PNd8 and PNd16 cortices was performed by measuring the intensity of Western blots, using the M2F6 monoclonal antibody that could recognize both the E and A isoforms (Fig. 12). In agreement with the decline of both the A and E isoforms of drebrin in the supernatant during development, the total drebrin intensity (drebrin A + drebrin E) in the supernatant fraction at PNd16 significantly decreased to 17.9 % of that at PNd8 ($P < 0.001$). In comparison, there was no significant difference in the actin intensity in the supernatant fraction between PNd8 and

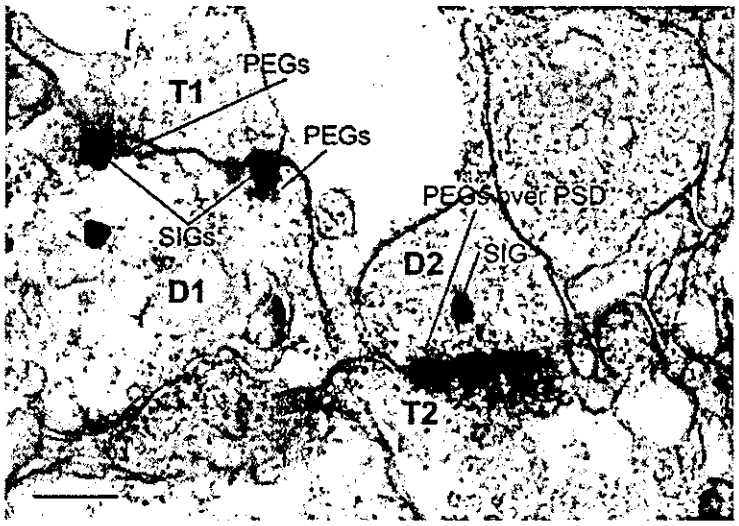

Fig. 8. Coexistence of drebrin A with the NR2B subunit of *N*-methyl-D-aspartate receptors at the postsynaptic membrane of a postnatal day (PNd) 7 dendrite. D1 to the left exhibits silver-intensified colloidal gold particles (SIG), reflecting immunoreactivity for drebrin A. Two of the SIG particles occur along the intracellular, postsynaptic membrane surface. Immediately adjacent to each of the SIG particles, two to four postembedding gold immunolabeling procedure (PEG) particles occur, reflecting the presence of low levels of NR2B subunits. The presynaptic terminal T1 contains only a few vesicles. In contrast, the terminal, T2, forming the adjacent synapse contains many vesicles, and the postsynaptic membrane of D2 exhibits a thick postsynaptic density (PSD). At least 12 PEG particles occur over the postsynaptic density, indicating the prevalence of NR2B subunits. This postsynaptic membrane does not show detectable levels of drebrin A. Instead, drebrin A immunoreactivity is slightly removed from the postsynaptic membrane. Scale bar = 200 nm.

PNd16. Also, in the crude homogenate or the pellet fraction, drebrin intensity did not change significantly between PNd8 and PNd16.

Based on previously published results, we surmised that the pellet fraction prepared after centrifugation at 200,000 × *g* represented the association of drebrin with F-actin (Ishikawa et al., 1994). Earlier studies had established that high salt could extract actin binding proteins from F-actin pellets (Glenney et al., 1982; Yamashiro-Matsumura and Matsumura, 1985). When this same procedure was used on our pellet fractions, a large portion of drebrin A was extracted from the pellet and entered the supernatant fraction (Fig 13). This outcome indicated that a large portion of drebrin A in the pellet was bound to the cytoskeleton and most likely to F-actin and microsomes and not to the plasma membrane.

DISCUSSION

The present study revealed a clear-cut segregation of drebrin A to postsynaptic sides of asymmetric synapses within mature cortex and hippocampus. During the phase of active synaptogenesis, drebrin A was present at the submembranous zone of dendritic plasma membranes before the formation of PSDs or spine heads, and also before the aggregation of vesicles presynaptically. This observation is consistent with results from our previous in vitro study, indicating that clustering of drebrin A precedes the formation of spines (Takahashi et al., 2003). Contrary to the presumptions we held before this ultrastructural study, our new observations indicate that drebrin E, *together with drebrin A*, are involved in the initial formation of protospines, rather than the involvement of drebrin E, alone. Moreover, the present ultrastructural study was able to verify that drebrin A occurs at membranous sites that were positively identifiable as synaptic, based on the emergence of a few vesicles, PSDs, and/or aggregation of glutamate receptor subunits there. The biochemical results indicate that the phase of synaptogenesis is paralleled by the increasing association of drebrin A with the pellet fraction containing actin. Below, we discuss the possibility that drebrin A may be involved in organizing the dendritic pool of actin for the formation of at least some of the spines and axospinous excitatory synapses.

Drebrin A is postsynaptic for excitatory synapses

The segregation of drebrin A to the postsynaptic side was clearer than it was for any of our previous observations of synaptic proteins, including the glutamatergic receptors (Aoki et al., 1994; Farb et al., 1995) and PSD-95 (Aoki et al., 2001). This was so, even though the immunolabeling for glutamatergic receptor subunits and PSD-95 faced similar technical limitations. We also noted absence of drebrin A at almost all of the mature symmetric synapses. Symmetric synapses are sites for inhibitory inputs, indicated by the clustering of $GABA_A$ receptor subunits, proteins such as gephyrin for the anchoring of these subunits and contacts formed by GABAergic axon terminals (reviewed by Fritschy and Brunig, 2003). Symmetric synapses also are associated with axons releasing neuromodulators, such as the monoamines and acetylcholine (Descarries, 1991).The segregation of labeling between symmetric and asymmetric synapses indicates that drebrin A is involved in the formation of at least some of the excitatory synapses but not of the GABAergic or purely modulatory synapses. Whether or not another organizer of F-actin occurs at GABAergic synapses remains unknown.

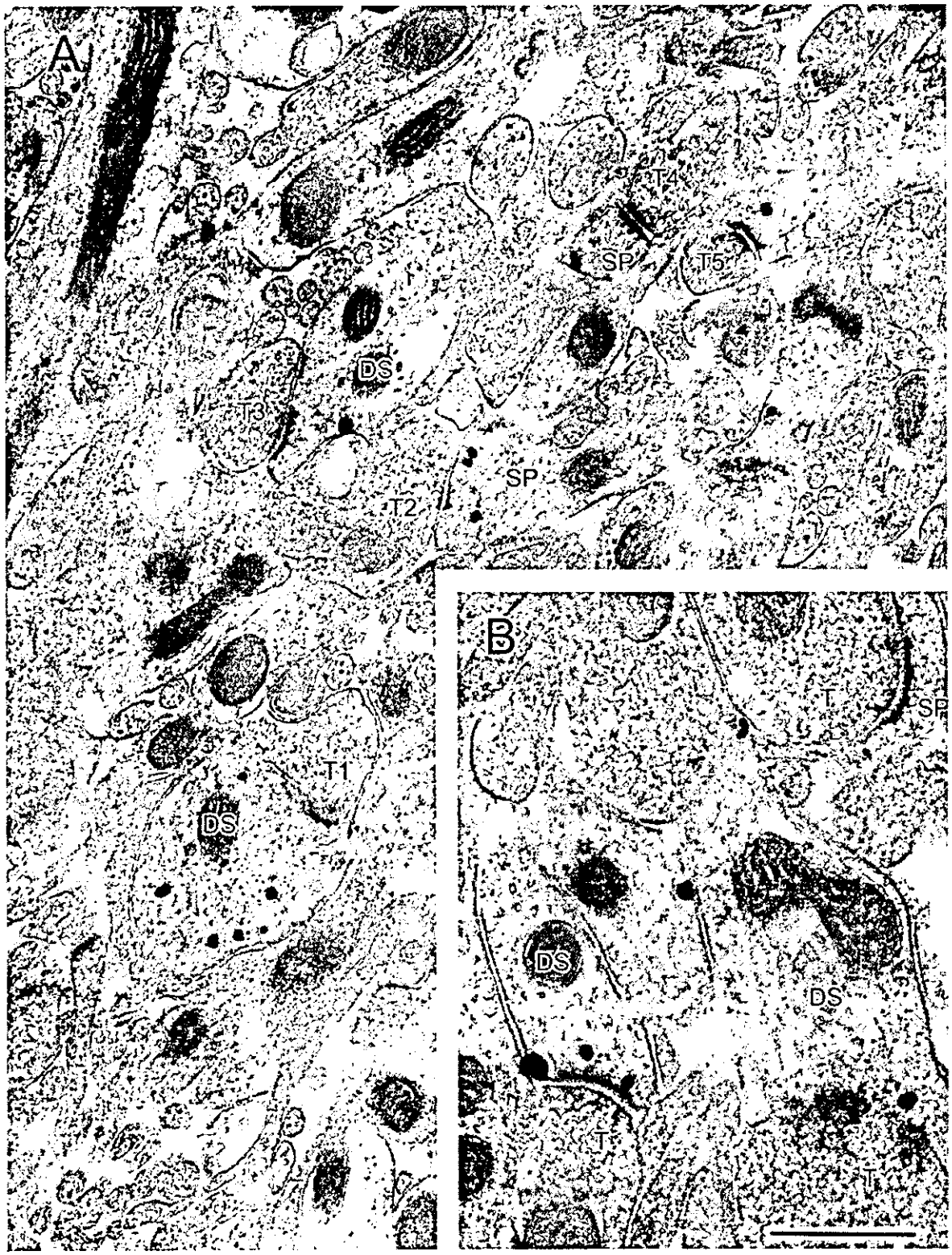

Fig. 9. Drebrin A in the synaptic neuropil of the molecular layer of the adult infrapyramidal dentate gyrus. Silver-intensified colloidal gold particles (SIG) were used to detect drebrin A. **A:** Five synapses, all asymmetric and associated with immunoreactivity to drebrin A on the postsynaptic side, only. The postsynaptic side is indicated as DS for dendritic shafts or as SP for spines, whereas the presynaptic profiles are indicated as T for terminal. At synapses formed with terminals T1, T2 and T3, the SIG particles occur along nonsynaptic portions of the plasma membrane and at the periphery of the postsynaptic density (PSD). At these synapses and all others, SIG particles occur in the cytoplasm as well. **B:** Three more synapses, two of which exhibit SIG particles discretely along the postsynaptic membrane. Additional SIG particles occur at nonjunctional sites. Scale bar = 666 nm in B; 500 nm for A.

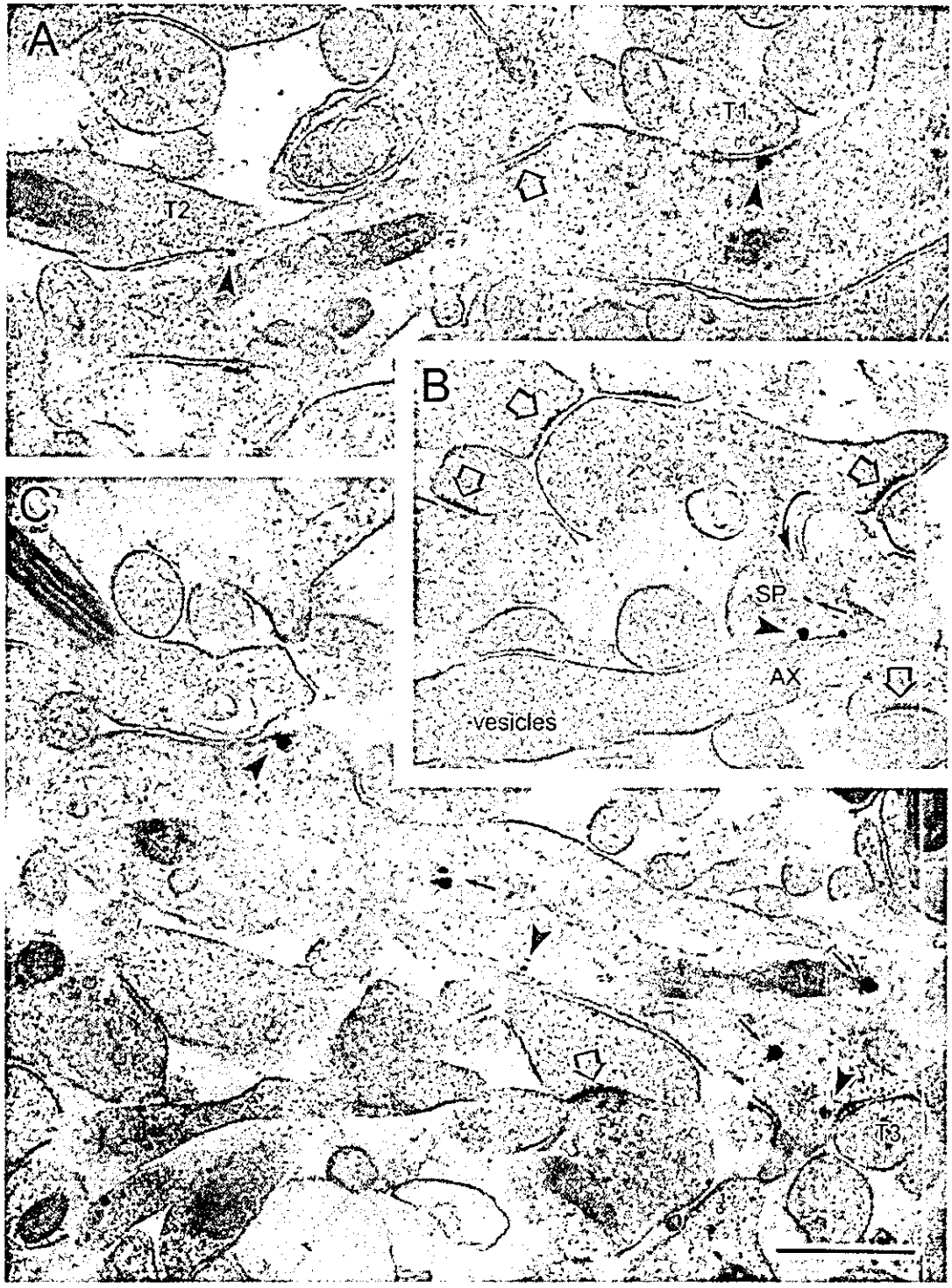

Fig. 10. Drebrin A in the molecular layer of postnatal day (PNd) 7 infrapyramidal dentate gyrus. Silver-intensified colloidal gold particles (SIG) were used as the label to detect the presence of drebrin A. **A:** Selective labeling along junctional portions of the plasma membrane. The arrowhead to the right shows SIG particles associated with a morphologically identifiable synapse (T1 marks the presynaptic terminal), whereas the SIG particle to the left shows no association with postsynaptic densities (PSDs). The immediately adjacent profile, T2, appears to be an axon terminal, indicating that this site is an immature synapse. The open arrow in the middle (and in other panels) points to a well-differentiated synapse lacking SIG particles. **B:** Three SIG particles occurring within a spine head (SP) lacking a PSD (arrowhead points to membranous SIG; small arrow to a cytoplasmic SIG). The immediately adjacent profile is an axon (Ax), as is evident by the cluster of vesicles in the same profile, toward the left. The same filopodia branches (curved arrow) from a more well-established but unlabeled spine with PSD (open arrows). **C:** A dendrite with irregular contours, no apparent microtubules, and containing six clusters of SIG particles. SIG occurs discretely along the plasma membrane forming a protuberance (arrowhead to the left) and contacting an axon. The arrowhead in the center points to an SIG particle along the plasma membrane that lacks apparent association with any axon. The arrowhead to the right points to the SIG particle associated with a portion of the plasma membrane beginning to form a PSD adjacent to an axon terminal, T. Arrows point to SIG particles in the cytoplasm, away from the plasma membrane. Scale bar = 500 nm in C (applies to A–C).

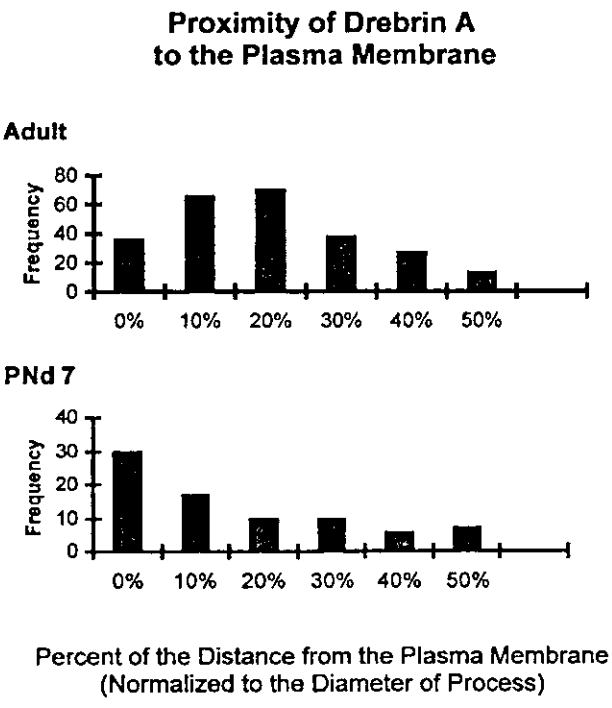

Fig. 11. Histograms showing the distribution of silver-intensified colloidal gold (SIG) particles in relation to the plasma membrane. The percentage values on the x-axis depict distances from the plasma membrane, normalized to the diameter of the profile in which the SIG particles are found. The y-axis depicts frequency of encounters at these varying distances from the membrane. Zero percent denotes SIG occurring at the plasma membrane. The encountered SIG particles were tallied from two postnatal day 7 and two adult hippocampal tissues.

Because GABAergic synapses occur at nonspinous portions of the plasma membrane, these synapses may not require F-actin binding proteins. Alternatively, a counterpart to an F-actin binding protein like drebrin may still be required at GABAergic synapses for the sake of receptor clustering and anchoring.

It has been shown previously that asymmetric synapses increase progressively in the neuropil during early postnatal development and that the spines emerge from stubby protospines along dendritic shafts after dendritic filopodia have disappeared (Vaughn, 1989; Harris, 1999; Jontes et al., 2000). Based on these observations, we surmise that PSDs convert from thin to thick during ontogeny, thereby converting synapses with symmetric appearances along protospines into those with asymmetric appearances at the spine heads. Our past (Aoki et al., 1994; Aoki, 1997) and present dual PEG immunocytochemical localization of glutamatergic receptor subunits corroborate this finding, because these receptors are found on synapses with very thin PSDs early on, and at progressively thicker PSDs in later weeks and in adulthood. The association of drebrin A with symmetric synapses at PNd7 and with asymmetric synapses in adulthood is likely to reflect drebrin A's association with newly formed glutamatergic synapses and of its persistence there during varying phases of maturation, rather than the switching of drebrin A from inhibitory to excitatory synapses during development. In support of this idea, drebrin A immunoreactivity was absent from symmetric synapses that had begun to acquire some of the morphological characteristics of mature GABAergic synapses (e.g., large cluster of vesicles that are associated along the presynaptic membrane; clearly defined microtubules within the postsynaptic dendrite, GABA immunoreactivity within the terminal). Drebrin A may be useful for identifying immature excitatory synapses before they acquire the more obvious morphological features. Studies are under way to determine whether the arrival of drebrin A to the dendritic membrane precedes arrival of NMDA receptor subunits or is linked to NMDA receptor recruitment.

Drebrin A arrives at dendritic membranes before synaptogenesis

By using both SIG and DAB as immunolabels for electron microscopy, we show that drebrin A appears at the earliest phase of synaptogenesis. Although neither label can be used to reveal the absolute values of drebrin A concentrations at junctions, the SIG label could be used to assess the relative concentration of antigens in the proximity of synaptic junctions. Our observations of tissue immunolabeled using HRP-DAB and SIG as the label indicate that the *proportion* of synaptic junctions lacking drebrin A immunoreactivity is greater at PNd7 than in adulthood. It has been reported that the turn-over rate of spines is higher in neonatal brain than in adult brain (Lendvai et al., 2000). It may be that drebrin A plays a role not only at the beginning of synaptogenesis and spinogenesis but also in the maintenance of spines. Once a spine loses drebrin A, that spine may be cleared from the neuropil more rapidly. If so, then the higher turnover rate of spines neonatally may be a consequence of a larger proportion of spines having lost drebrin A. Further experiments are needed to link physiological characteristics of spines to the presence of drebrin A and of the cause–effect relationship between spine turnover and drebrin A content.

Possible role of Drebrin A in neonatal cortex and hippocampus

In this study, we show that the rapid increase of drebrin A is paralleled by the disappearance of drebrin from the supernatant fraction at PNd8. Because we prepared crude homogenates in the presence of a mild detergent, NP-40, we expect the supernatant fraction to contain proteins that are free in the cytosol or solubilized from the membrane. Although G-actin (actin monomers) occurs in high amounts in the supernatant, we know that drebrin does not associate with actin monomers (Ishikawa et al., 1994). Thus, drebrin in the supernatant could represent free drebrin and those loosely attached to the plasma membrane. This interpretation agrees well with the SIG labeling PATTERN, which showed membranous labeling for drebrin A more at PNd7 than in adulthood. The drebrin appearing in the supernatant may be the correlate of ultrastructurally observed junctional and nonjunctional drebrin at flat portions and shallow protrusions (protospines) along intracellular surfaces of dendritic membranes.

The extraction experiment shows that drebrin's association with the pellet is ionic and nonmembranous. The best candidate for an element contained within pellets

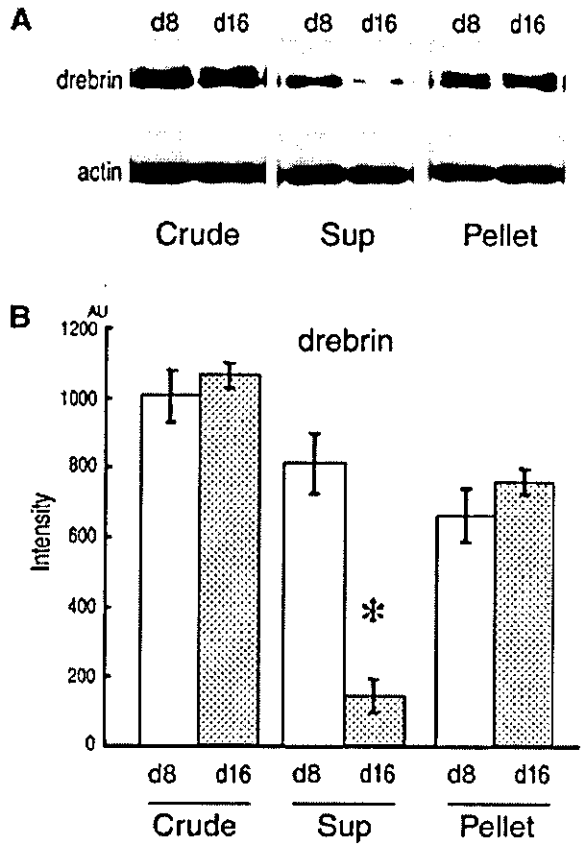

Fig. 12. Densitometric analysis of drebrin in each subcellular fraction. Each fraction equivalent to 0.23 mg of wet weight tissue was quantitatively analyzed in Western blots for drebrin content. Drebrin content was measured as intensity in Western blots from the crude, supernatant, and pellet fractions of postnatal day (PNd) 8 and PNd16 cortex homogenates. Panel A shows an example of a Western blot using M2F6 monoclonal antibody directed against drebrin and β-actin immunostaining used for comparison. Drebrin intensity in the supernatant fraction at PNd16 (d16) was significantly less than that at PNd8 (d8, n = 4, $*P < 0.001$, t test). Drebrin intensity in the crude and pellet fractions did not change during the same developmental period (n = 4; $P = 0.42$ for crude fraction; n = 4; $P = 0.30$ for the pellet fraction). AU, Arbitrary unit. Error bars indicate SEM. Histograms show mean values ± SEM.

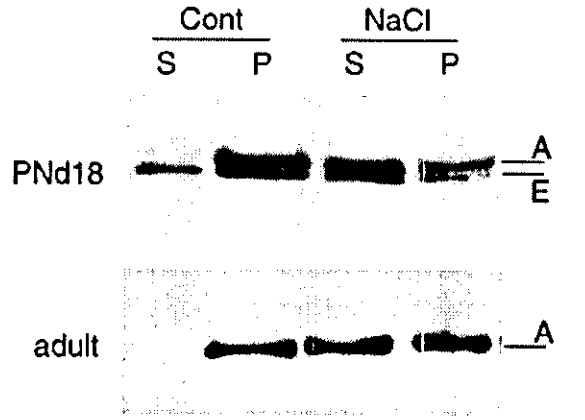

Fig. 13. Drebrin is bound to the cytoskeleton in the pellet. Crude fractions were prepared from cerebral cortices of postnatal day (PNd) 18 (upper panel) and adult rats (lower panel) and was the centrifuged at 200,000 × g for 60 minutes at 4°C. The resultant pellet was then homogenized in high-salt buffer and recentrifuged. Proteins in each fraction equivalent to equal amount of wet weight tissue (0.23 mg) were analyzed by Western blot using the M2F6 antibody. Note that intense bands in the supernatant fraction appeared in the high-salt buffer. A, drebrin A; E, drebrin E.

that can provide ionic and nonmembranous association is the cytoskeletal matrix (Glenney et al., 1982; Yamashiro-Matsumura and Matsumura, 1985), of which F-actin is the main constituent within mature spines (Matus, 2000). Drebrin associated with F-actin in the pellet may be the component involved in the formation of spines from the shallow protrusions (protospines).

How does drebrin A associated with F-actin promote spine formation? In vitro assays have shown that drebrin reduces the association of F-actin with α-actinin and tropomyosin, possibly by binding competitively to these latter proteins' binding sites to actin (Shirao and Sekino, 2001). Because α-actinin mediates cross-linking and bundling of actin filaments, the consequence of drebrin binding to F-actin within the submembranous zone would be to relax the actin cytoskeletal matrix, thereby allowing for shape changes to take place. Flexibility is exactly what would be needed for the formation and retraction of dendritic filopodia, enabling actin-based shape changes to occur there.

Our recent and older observations indicate that drebrin A may also play a role at the initial event of synaptogenesis, that is, contact between an axon and a dendrite, even before it plays a role in spine formation. The new observation supporting this idea is that drebrin A immunoreactivity could be found along the flat submembranous surfaces of dendrites and at protospines. This finding is corroborated by earlier studies analyzing the role of drebrin upon intercellular adhesion of cells grown in culture. Specifically, Ikeda et al. (1996) observed that drebrin A transfection of fibroblasts led to the stabilization of adhesion plaques. The isoform drebrin E has been observed to interact with connexin at sites of functional GAP junctions within brain tissue (Butkevich et al., 2004) and also to occur at junctional plaques, defining a specific microfilament anchorage system in polar epithelial cells (Peitsch et al., 1999). There is additional evidence indicating that drebrin A may recruit synaptic proteins resident in spines. Interactions between PSDs and the postsynaptic cytoskeleton involve Shank, a scaffold protein (Naisbitt et al., 1999). Shank is reported to promote the maturation of dendritic spines by regulating the accumulation of spine-resident proteins, such as PSD-95, F-actin, and the NR1 subunit of NMDA receptors (Sala et al., 2001). This influence of Shank upon spine maturation, in turn, is dependent on its binding to Homer. We have shown that drebrin A, like Shank, promotes the accumulation of PSD-95 (Takahashi et al., 2003). Because Homer binds to drebrin A (Mizutani et al., 1999) as well as to Shank, drebrin A may facilitate the synaptic recruitment of Homer and Shank and, hence, the accumulation of PSD-95 and receptors for a coordinated maturation of spines and synapses.

Possible role of drebrin A in adulthood

The developmental increase of drebrin A's association with the pellet fraction and, thus, with actin indicates that drebrin A may continue to regulate dendritic shape in adulthood. Recent studies have permitted direct visualization of spines in vivo over a period of days. Such studies have shown that, indeed, spines undergo turnover throughout adulthood, with approximately 20% of those in the adult cortex disappearing within a day (Trachtenberg et al., 2002; Majewska and Sur, 2003). Spinogenesis is even more active in the hippocampus, with profound changes in spine density occurring every 4–5 days, in synchrony with the estrous cycle (Gould et al., 1990; Woolley et al., 1990; Leranth et al., 2004). The same studies and many others (Bonhoeffer and Yuste, 2002; Star et al., 2002; Konur and Yuste, 2004) have also shown that spine motility is dependent on synaptic activity (reviewed by Harris, 1999). Studies are planned that will examine the impact of overexpression and loss of expression of drebrin A and/or drebrin E upon spine and synapse formation.

ACKNOWLEDGMENTS

We thank Dr. Robert Levy for critical reading of the article and for helpful discussions.

LITERATURE CITED

Aoki C. 1997. Postnatal changes in the laminar and subcellular distribution of NMDA-R1 subunits in the cat visual cortex as revealed by immuno-electron microscopy. Brain Res Dev Brain Res 98:41–59.

Aoki C, Venkatesan C, Go CG, Mong JA, Dawson TM. 1994. Cellular and subcellular localization of NMDA-R1 subunit immunoreactivity in the visual cortex of adult and neonatal rats. J Neurosci 14:5202–5222.

Aoki C, Rodrigues S, Kurose H. 2000. Use of electron microscopy in the detection of adrenergic receptors. Methods Mol Biol 126:535–563.

Aoki C, Miko I, Oviedo H, Mikeladze-Dvali T, Alexandre L, Sweeney N, Bredt DS. 2001. Electron microscopic immunocytochemical detection of PSD-95, PSD-93, SAP-102, and SAP-97 at postsynaptic, presynaptic, and nonsynaptic sites of adult and neonatal rat visual cortex. Synapse 40:239–257.

Asada H, Uyemura K, Shirao T. 1994. Actin-binding protein, drebrin, accumulates in submembranous regions in parallel with neuronal differentiation. J Neurosci Res 38:149–159.

Bonhoeffer T, Yuste R. 2002. Spine motility. Phenomenology, mechanisms, and function. Neuron 35:1019–1027.

Butkevich E, Hulsmann S, Wenzel D, Shirao T, Duden R, Majoul I. 2004. Drebrin is a novel connexin-43 binding partner that links gap junctions to the submembrane cytoskeleton. Curr Biol 14:650–658.

Crosbie R, Adams S, Chalovich JM, Reisler E. 1991. The interaction of caldesmon with the COOH terminus of actin. J Biol Chem 266:20001–20006.

Descarries L. 1991. Non junctional relationships of monoamine axon terminals in the cerebral cortex of adult rat. Volume transmission in the brain: novel mechanisms for neural transmission. Adv Neurosci 1:53–62.

Erisir A, Levey AI, Aoki C. 2001. Muscarinic receptor M(2) in cat visual cortex: laminar distribution, relationship to gamma-aminobutyric acidergic neurons, and effect of cingulate lesions. J Comp Neurol 441:168–185.

Farb CR, Aoki C, Ledoux JE. 1995. Differential localization of NMDA and AMPA receptor subunits in the lateral and basal nuclei of the amygdala: a light and electron microscopic study. J Comp Neurol 362:86–108.

Fox JE. 1985. Identification of actin-binding protein as the protein linking the membrane skeleton to glycoproteins on platelet plasma membranes. J Biol Chem 260:11970–11977.

Fritschy JM, Brunig I. 2003. Formation and plasticity of GABAergic synapses: physiological mechanisms and pathophysiological implications. Pharmacol Ther 98:299–323.

Fujisawa S, Aoki C. 2003. In vivo blockade of N-methyl-D-aspartate receptors induces rapid trafficking of NR2B subunits away from synapses and out of spines and terminals in adult cortex. Neuroscience 121:51–63.

Glenney JR Jr, Glenney P, Weber K. 1982. F-actin-binding and cross-linking properties of porcine brain fodrin, a spectrin-related molecule. J Biol Chem 257:9781–9787.

Gould E, Woolley CS, Frankfurt M, McEwen BS. 1990. Gonadal steroids regulate dendritic spine density in hippocampal pyramidal cells in adulthood. J Neurosci 10:1286–1291.

Harris KM. 1999. Structure, development, and plasticity of dendritic spines. Curr Opin Neurobiol 9:343–348.

Hayashi K, Shirao T. 1999. Change in the shape of dendritic spines caused by overexpression of drebrin in cultured cortical neurons. J Neurosci 19:3918–3925.

Hayashi K, Ishikawa R, Ye LH, He XL, Takata K, Kohama K, Shirao T. 1996. Modulatory role of drebrin on the cytoskeleton within dendritic spines in the rat cerebral cortex. J Neurosci 16:7161–7170.

Hayashi K, Suzuki K, Shirao T. 1998. Rapid conversion of drebrin isoforms during synapse formation in primary culture of cortical neurons. Brain Res Dev Brain Res 111:137–141.

He Y, Janssen WG, Morrison JH. 1998. Synaptic coexistence of AMPA and NMDA receptors in the rat hippocampus: a postembedding immunogold study. J Neurosci Res 54:444–449.

Ikeda K, Shirao T, Toda M, Asada H, Toya S, Uyemura K. 1995. Effect of a neuron-specific actin-binding protein, drebrin A, on cell-substratum adhesion. Neurosci Lett 194:197–200.

Ikeda K, Kaub PA, Asada H, Uyemura K, Toya S, Shirao T. 1996. Stabilization of adhesion plaques by the expression of drebrin A in fibroblasts. Brain Res Dev Brain Res 91:227–236.

Imamura K, Shirao T, Mori K, Obata K. 1992. Changes of drebrin expression in the visual cortex of the cat during development. Neurosci Res 13:33–41.

Ishikawa R, Hayashi K, Shirao T, Xue Y, Takagi T, Sasaki Y, Kohama K. 1994. Drebrin, a development-associated brain protein from rat embryo, causes the dissociation of tropomyosin from actin filaments. J Biol Chem 269:29928–29933.

Jontes JD, Buchanan J, Smith SJ. 2000. Growth cone and dendrite dynamics in zebrafish embryos: early events in synaptogenesis imaged in vivo. Nat Neurosci 3:231–237.

Kojima N, Shirao T, Obata K. 1993. Molecular cloning of a developmentally regulated brain protein, chicken drebrin A and its expression by alternative splicing of the drebrin gene. Brain Res Mol Brain Res 19:101–114.

Konur S, Yuste R. 2004. Developmental regulation of spine and filopodial motility in primary visual cortex: reduced effects of activity and sensory deprivation. J Neurobiol 59:236–246.

Lendvai B, Stern EA, Chen B, Svoboda K. 2000. Experience-dependent plasticity of dendritic spines in the developing rat barrel cortex in vivo. Nature 404:876–881.

Leranth C, Hajszan T, MacLusky NJ. 2004. Androgens increase spine synapse density in the CA1 hippocampal subfield of ovariectomized female rats. J Neurosci 24:495–499.

Levy RB, Aoki C. 2002. Alpha7 nicotinic acetylcholine receptors occur at postsynaptic densities of AMPA receptor-positive and -negative excitatory synapses in rat sensory cortex. J Neurosci 22:5001–5015.

Majewska A, Sur M. 2003. Motility of dendritic spines in visual cortex in vivo: changes during the critical period and effects of visual deprivation. Proc Natl Acad Sci U S A 100:16024–16029.

Marty S, Wehrle R, Alvarez-Leefmans FJ, Gasnier B, Sotelo C. 2002. Postnatal maturation of Na+, K+, 2Cl- cotransporter expression and inhibitory synaptogenesis in the rat hippocampus: an immunocytochemical analysis. Eur J Neurosci 15:233–245.

Matus A. 2000. Actin-based plasticity in dendritic spines. Science 290:754–758.

Megias M, Emri Z, Freund TF, Gulyas AI. 2001. Total number and distribution of inhibitory and excitatory synapses on hippocampal CA1 pyramidal cells. Neuroscience 102:527–540.

Minelli A, Alonso-Nanclares L, Edwards RH, DeFelipe J, Conti F. 2003. Postnatal development of the vesicular GABA transporter in rat cerebral cortex. Neuroscience 117:337–346.

Mizutani A, Shiraishi Y, Mikoshiba K, Furuichi T. 1999. Characterization of Cupidin-binding proteins. Soc Neurosci Abst 25:805.807.

Naisbitt S, Kim E, Tu JC, Xiao B, Sala C, Valtschanoff J, Weinberg RJ, Worley PF, Sheng M. 1999. Shank, a novel family of postsynaptic

density proteins that binds to the NMDA receptor/PSD-95/GKAP complex and cortactin. Neuron 23:569–582.

Peitsch WK, Grund C, Kuhn C, Schnolzer M, Spring H, Schmelz M, Franke WW. 1999. Drebrin is a widespread actin-associating protein enriched at junctional plaques, defining a specific microfilament anchorage system in polar epithelial cells. Eur J Cell Biol 78:767–778.

Peters A. 2002. Examining neocortical circuits: some background and facts. J Neurocytol 31:183–193.

Petralia RS, Wenthold RJ. 1992. Light and electron immunocytochemical localization of AMPA-selective glutamate receptors in the rat brain. J Comp Neurol 318:329–354.

Phend KD, Rustioni A, Weinberg RJ. 1995. An osmium-free method of Epon embedment that preserves both ultrastructure and antigenicity for post-embedding immunocytochemistry. J Histochem Cytochem 43: 283–292.

Purpura DP, Pappas GD. 1972. Structure and function of synapses. New York: Raven Press.

Sala C, Piech V, Wilson NR, Passafaro M, Liu G, Sheng M. 2001. Regulation of dendritic spine morphology and synaptic function by Shank and Homer. Neuron 31:115–130.

Shirao T. 1995. The roles of microfilament-associated proteins, drebrins, in brain morphogenesis: a review. J Biochem (Tokyo) 117:231–236.

Shirao T, Sekino Y. 2001. Clustering and anchoring mechanisms of molecular constituents of postsynaptic scaffolds in dendritic spines. Neurosci Res 40:1–7.

Shirao T, Obata K. 1986. Immunochemical homology of 3 developmentally regulated brain proteins and their developmental change in neuronal distribution. Dev Brain Res 29:233–244.

Shirao T, Inoue HK, Kano Y, Obata K. 1987. Localization of a developmentally regulated neuron-specific protein S54 in dendrites as revealed by immunoelectron microscopy. Brain Res 413:374–378.

Shirao T, Kojima N, Kato Y, Obata K. 1988. Molecular cloning of a cDNA for the developmentally regulated brain protein, drebrin. Brain Res 464:71–74.

Shirao T, Kojima N, Nabeta Y, Obata K. 1989. Two forms of drebrins, developmentally regulated brain proteins, in rat. Proc Jpn Acad 65: 169–172.

Shirao T, Kojima N, Obata K. 1992. Cloning of drebrin A and induction of neurite-like processes in drebrin-transfected cells. Neuroreport 3:109–112.

Shirao T, Hayashi K, Ishikawa R, Isa K, Asada H, Ikeda K, Uyemura K. 1994. Formation of thick, curving bundles of actin by drebrin A expressed in fibroblasts. Exp Cell Res 215:145–153.

Star EN, Kwiatkowski DJ, Murthy VN. 2002. Rapid turnover of actin in dendritic spines and its regulation by activity. Nat Neurosci 5:239–246.

Takahashi H, Sekino Y, Tanaka S, Mizui T, Kishi S, Shirao T. 2003. Drebrin-dependent actin clustering in dendritic filopodia governs synaptic targeting of postsynaptic density-95 and dendritic spine morphogenesis. J Neurosci 23:6586–6595.

Trachtenberg JT, Chen BE, Knott GW, Feng G, Sanes JR, Welker E, Svoboda K. 2002. Long-term in vivo imaging of experience-dependent synaptic plasticity in adult cortex. Nature 420:788–794.

Vaughn JE. 1989. Fine structure of synaptogenesis in the vertebrate central nervous system. Synapse 3:255–285.

Woolley CS, Gould E, Frankfurt M, McEwen BS. 1990. Naturally occurring fluctuation in dendritic spine density on adult hippocampal pyramidal neurons. J Neurosci 10:4035–4039.

Yamashiro-Matsumura S, Matsumura F. 1985. Purification and characterization of an F-actin-bundling 55-kilodalton protein from HeLa cells. J Biol Chem 260:5087–5097.

Available online at www.sciencedirect.com
SCIENCE DIRECT®
Neuroscience Research 49 (2004) 205–217
Neuroscience Research
www.elsevier.com/locate/neures

Antisense knockdown of drebrin A, a dendritic spine protein, causes stronger preference, impaired pre-pulse inhibition, and an increased sensitivity to psychostimulant

Rika Kobayashi [a], Yuko Sekino [b], Tomoaki Shirao [b], Satoshi Tanaka [b], Taichi Ogura [a], Ken Inada [c], Makoto Saji [a,d,*]

[a] *Division of Brain Science, Kitasato University Graduate School of Medical Sciences, Sagamihara 228-8555, Japan*
[b] *Department of Neurobiology and Behavior, Gunma University School of Medicine, Maebashi 371-8511, Japan*
[c] *Department of Psychiatry, Kitasato University School of Medicine, Sagamihara 288-8555, Japan*
[d] *Department of Physiology, Kitasato University School of Allied Health Sciences, Sagamihara 288-8555, Japan*

Received 7 January 2004; accepted 25 February 2004

Available online 24 April 2004

Abstract

Drebrin located in dendritic spines regulates their morphological changes and plays a role in the synaptic plasticity via spine function. Reduced drebrin has been found in the brain of patients with Alzheimer's disease or Down's syndrome. To examine whether the down-regulation of drebrin protein levels causes deficits in higher brain function, such as memory or cognition, we performed antisense-induced knockdown of drebrin A expression in rat brain using an hemagglutinating virus of Japan (HVJ)-liposome gene transfer technique. We investigated the effects of drebrin in vivo knockdown on spatial memory in a water-maze task, sensorimotor gating in a pre-pulse-inhibition test, adaptive behaviors in an open-field test, and sensitivity to psychostimulant in an amphetamine-induced locomotor response. Rats with drebrin A in vivo knockdown displayed a stronger preference for a previous event due to perseverative behavior, impaired pre-pulse inhibition (PPI), increased locomotor activity, anxiety-like behavior, and an increased sensitivity to psychostimulant, suggesting behaviors related to schizophrenia. These findings indicated that decreased drebrin produces deficits in cognitive function but not in spatial memory, probably via hypofunction of dendritic spines.

Keywords: Actin-binding protein; Antisense oligodeoxynucleotides; HVJ-liposome-mediated gene transfer; Water-maze task; Locomotor activity; Cognitive function

1. Introduction

Many types of neurons have dendrites with small protrusions termed spines. In the cerebral cortex, about 75% of neurons have dendrites with a high density of spines, and most of these spiny neurons are excitatory (Keller, 2002). Furthermore, most of the excitatory synapses in the cortex make contact with the dendritic spines of other excitatory neurons (Marrs et al., 2001; Okabe et al., 2001). Since dendritic spines are specialized compartments that serve as the structural base for synaptic signaling, integration, and plasticity in mature brain, the ability of spines to alter their shape or length and the stability of synaptic contacts at spines provide a powerful mechanism for synaptic plasticity in the excitatory circuitry in the cerebral cortex and the limbic regions, such as the hippocampus and the amygdala (Engert and Bonhoeffer, 1999; Lendvai et al., 2000; Shirao and Sekino, 2001).

Drebrin A, an actin-binding protein, accumulates specifically in the dendritic spines (Hayashi et al., 1996; Shirao et al., 1987; Shirao, 1995). In recent in vitro studies, it has been demonstrated that drebrin A regulates changes in the shape and density of dendritic spines, probably via the rearrangement of cytoskeletal actin filaments (Hayashi and Shirao, 1999; Shirao et al., 1994). In particular, high expression of drebrin A is specifically observed in the cerebral cortex, hippocampus, amygdala, thalamus, and striatum (Hayashi et al., 1996; Shirao and Obata, 1986), which are responsible

* Corresponding author. Tel.: +81-427-78-8311; fax: +81-427-78-8153.
E-mail address: sajim@ahs.kitasato-u.ac.jp (M. Saji).

0168-0102/$ – see front matter © 2004 Elsevier Ireland Ltd and The Japan Neuroscience Society. All rights reserved.
doi:10.1016/j.neures.2004.02.014

for higher brain functions. Clinically, a marked decrease of drebrin A was found in brains with Alzheimer's disease (Harigaya et al., 1996; Hatanpaa et al., 1999) or Down's syndrome (Shim and Lubec, 2002). The synaptic plasticity of the excitatory circuitry underlying higher brain functions, such as learning, memory, or cognition is considered to involve a stimulus-dependent change of the shape and density of dendritic spines (Keller, 2002; Marrs et al., 2001; Okabe et al., 2001; Shirao and Sekino, 2001). Therefore, it is hypothesized that experimentally induced knockdown of drebrin A, dendritic spine protein, in the whole brain could cause some defects in memory formation, sensorimotor gating function, or cognitive function.

To examine whether the dysfunction or hypofunction of dendritic spine-mediated synaptic function in the excitatory circuitry in the forebrain causes defects in spatial reference memory, adaptive response to a novel environment, and sensorimotor gating, we performed antisense-induced down-regulation of drebrin A expression in the forebrain regions. In rats with long-lasting knockdown of drebrin A expression in the forebrain regions, such as the neocortex or hippocampus, we tested spatial learning using the Morris water-maze task, an adaptive response to a novel environment in an open-field test, psychostimulant sensitivity using an amphetamine-induced locomotor response, and sensorimotor gating function in the pre-pulse inhibition (PPI) test of the acoustic startle response, all of which are sensitive to anti-glutaminergic drugs and lesions of the hippocampus (Bakshi and Geyer, 1998; Carlsson and Carlsson, 1990; Ellison, 1995; Morris et al., 1982). To achieve a long-lasting in vivo knockdown of drebrin A expression by a single intra-ventricular injection of antisense oligodeoxynucleotides (ODNs), we chose to use a combination of the antisense technique and the hemagglutinating virus of Japan (HVJ)-liposome-mediated gene transfer method. HVJ-liposome-mediated gene transfer is a method that enables delivery of the contents (ODNs) of the HVJ-liposome vector directly into cells by means of the Sendai virus (HVJ)-cell fusion machinery (Inada et al., 2003; Iwakuma et al., 2003; Kobayashi et al., 2002; Saeki et al., 1997; Yamada et al., 1996). Down-regulation of drebrin A by the antisense ODNs we used in the present study has induced the attenuation of synaptic clustering of PSD-95 as well as clustering of drebrin and F-actin in cultured hippocampal neurons (Takahashi et al., 2003).

2. Materials and methods

2.1. Animal care

Ninety six naïve, 10-week-old, male Wistar rats weighing 230–280 g (Japan SLC, Kanagawa, Japan) were used in the present study. The animals were housed in clear plastic cages in groups of two or three and were allowed access to food and water throughout the experiment. The animals were maintained in a temperature-, humidity-, and light-controlled environment with a 12 h light/dark cycle. On arrival in the colony, the experimenter holds the animal gently by the body rubbing its head and back for about 5 min. Not to be in fear of the experimenter, this type of handling was performed once a day for several days or a week until the surgical operation for the intra-ventricular injection of HVJ-liposomes containing ODNs was conducted.

All experiments conformed to Japanese and international guidelines on the ethical use of animals, and every effort was made to minimize the number of animals and their suffering.

2.2. Oligodeoxynucleotides (ODNs)

Phosphotioated ODNs (24 mers) corresponding to a specific segment in the 5′-coding region of drebrin cDNA were designed to selectively deacrese byosynthesis of the drebrin A as antisense ODNs to drebrin A (Dre-AS: 5′-AGGA-AGGCCCACTGTCCGATGCCT-3′)(Takahashi et al., 2003; Tanaka et al., 2001). Reversed antisense ODNs (Dre-RE: 5′-TCCGTAGCCTGTCACCCGGAAGGA-3′), in which the bases of the 24 mers corresponding to Dre-AS were reversed, were synthesized for use as a control. A search of the Genebank/EMBL database determined that none of the ODN sequence overlapped with other mammalian sequences.

2.3. Preparation of HVJ-liposome containing ODNs

The detailed preparation of anionic HVJ-liposome containing ODNs has been described elsewhere (Iwakuma et al., 2003; Saeki et al., 1997; Yamada et al., 1996). Briefly, three kinds of lipids (phosphatidylserine, phosphatidylcholine, and cholesterol) dissolved in chloroform (1 mg/ml) were mixed in a weight ratio of 1:4.8:2. One milligram of the lipid mixture was transferred into a glass tube and dried as a thin lipid film using a rotary evaporator filled with nitrogen gas at 40 °C. The lipid thin film layering on the bottom of a glass tube was hydrated in 200 μl of a balanced salt solution (BSS: 137 mM NaCl, 5.4 mM KCl, 10 mM Tris–HCl, pH 7.5) containing 100 μg of ODNs which were dispersed in the aqueous phase at room temperature. The mixture of the hydrated lipid thin film and ODNs was agitated by vortexing for 30 s and then incubated at 37 °C for 30 s. This procedure was repeated eight times, making fragments of lipid thin film into liposomes in which ODNs were packaged up. The liposome suspension was sonicated for 20 s and vortexed for 30 s. Then 300 μl of BSS was added to the liposomes suspension and incubated at 37 °C for 30 min shaking. The liposome suspension prepared above (500 μl) was mixed with 1 ml HVJ suspension (more than 10,000 hemagglutinating units), whose RNA genome had been inactivated by ultraviolet irradiation (198 mJ/cm^2) just before use. The mixture was incubated at 4 °C for 10 min and at 37 °C for 1 h shaking to facilitate the fusion between the inactivated HVJ and the liposomes. The ODNs–HVJ–liposome complex was loaded onto a discontinuous sucrose gradient and

centrifuged at 25,000 rpm at 4 °C for 1.5 h to separate the ODNs–HVJ–liposome complex from free HVJ. The purified ODNs–HVJ–liposomes suspension was adjusted to OD 1.0 (540 nm) with 200–250 μl of BSS. Since 10–30% of ODNs (10–30 μg) are available for packing into the liposomes (Kaneda, 1999), it is estimated that 1 μl of the purified ODNs–HVJ–liposomes (OD 1.0) contains about 40–120 ng of ODNs.

2.4. Intra-ventricular injection of an HVJ-liposome vector containing ODNs

Rats were anesthetized with an intra-peritoneal injection of pentobarbital sodium (40 mg/kg). A total of 30 μl (1.2–3.6 μg ODNs) of HVJ-liposome vectors containing ODNs was stereotaxically injected into both sides of the lateral ventricle in the rats. The coordinates for intra-ventricular injection in mm in respect to ear bar were; (1) AP: 8.2; L: +1.4; D: 3.8 and (2) AP: 8.2; L: −1.4; D: 3.8. A glass micropipette (tip size: 30–40 μm; volume: 2.5 μl/mm) made from a disposable micropipette (20 μl, Drummond), which was connected to an air pressure system with polyethylene tubing, was used for a single intra-ventricular injection of the HVJ-liposome vectors containing ODNs (Iwakuma et al., 2003).

2.5. Western blot analysis

For quantification of the protein expression levels, Western blot analysis was used. Rats were anesthetized with diethyl ether and decapitated at various days after the intra-ventricular injection of HVJ-liposome vectors containing antisense ODNs or reversed antisense ODNs. The hippocampus, neocortex, cerebellum and thalamus were quickly dissected out of the removed brain and stored at −80 °C before use. The tissue (100 μg per 1 μl buffer) was sonicated in cold sample buffer containing 40% glycerol, 20% Tris-glycine, 2% sodium dodecylsulfate (SDS), 5% 2-mercaptoethanol until the homogenate was uniform. The homogenate was centrifuged at 15,000 rpm for 10 min at 4 °C and denatured for 3 min. The supernatant of 4 μl was loaded on 8% sodium dodecylsulfate–polyacrylamide gel (40 μg protein per lane) and separated by electrophoresis. Separated proteins were transferred electrophoretically from the gel to a polyvinylidine difluoride (PVDF) membrane (ATTO, Tokyo, Japan). After being blocked with blocking buffer (Block Ace, Dainihon Seiyaku, Japan) at 4 °C for 1 h for drebrin A or overnight for β-actin, the membrane was processed with the primary antibodies overnight at room temperature for more than 1 h. Two primary antibodies were used, a rabbit polyclonal antibody against drebrin A (1:1000, produced by Dr. T Shirao) (Shirao et al., 1994) and a monoclonal antibody against β-actin (1:3000, Abcom, UK). After being washed in PBS containing 0.1% Tween for 1 h, the membrane was incubated with the second antibody, peroxidase-conjugated goat anti-rabbit IgG (1:2000 for drebrin A, 1:10000 for β-actin, Leinco Technologies) at room temperature for 1 h. Then the membrane was processed with enhanced chemiluminescence reagents to visualize the antibody reaction using an ECL detection kit (Amersham International, UK) and finally exposed to X-ray film (Kodak). Western blots were analyzed with computer densitometory by using NIH image software for quantification of drebrin A protein levels. For the measurement of β-actin as control protein, the membrane was reprobed with monoclonal antibody against β-actin to confirm equal protein loading in each lane. The mean optical densities of bands for two samples per animal were determined, and the film background was subtracted. The band densities for drebrin A or β-actin protein in treated rats were represented as relative percentages of those in non-treated control rats. The mean band densities thus obtained were statistically analyzed with one-way ANOVA and post-hoc Fisher's test to determine the significance.

2.6. Open field test for spontaneous locomotor activity, adaptive behaviors and amphetamine-induced locomotor response

A rat was placed in the center of a white square box (width, 1.0 m; height, 0.4 m). The locomotor behavior of the rat was recorded by a video camera during the initial 30 min period following the start of spontaneous locomotion in the open field. In experiment for psychostimulant-sensitivity, the locomotor behavior of the rat was recorded during the total 90 min period that consists of the initial 30 min period (pre-injection) after the start of spontaneous locomotion and the following 60 min period (post-injection) of amphetamine-induced locomotor response by the intra-peritoneal administration of amphetamine (1.0 mg/kg). From the 30 min or 90 min recording of locomotor behavior, rat position was tracked by computer and the locomotor distance during every 5 min period was measured as a locomotor activity using computer-guided image software (Kurihara Medical Instrument, Tokyo).

As for typical behaviors in adaptive response to a novel environment, a total duration of being stationary, being exploratory or grooming during the 30 min test period was measured from the 30 min recording of behaviors following the start of spontaneous locomotion in an open field, respectively. Being exploratory means both horizontal locomotion and vertical locomotion including rearing, while being stationary is defined as a stationary state without grooming or rearing.

2.7. Prepulse inhibition test of acoustic startle response

A startle chamber with a floor equipped with an electric weighing machine and a speaker mounted 24 cm above the floor for presenting acoustic noise burst was used. Rats were placed in the startle chamber and allowed to acclimate for 5 min before the test session. Background noise

was set at 65 dB of white noise throughout the acclimation period and test session. In a test session, 10 trials of three types of acoustic stimulation (total 30 trials) were given in pseudo-random order after initial startle-stimuli (20 ms burst of 120 dB). One of the three types was a startle pulse alone (P alone) trail, which involved a 20 ms burst of 120 dB, and the other two types were a combined trial of prepulse and startle pulse (PP70 &P and PP80 &P), which involved a 20 ms burst of 70 dB or 80 dB as a prepulse, respectively, followed by the same pulse as in the P alone trial 100 ms later. The inter-trial intervals averaged 40 s (20–60 s) were given in pseudo-random order. In addition to these three types of trials, no-stimulus (non-stim) trials were inserted between trials to check the baseline amplitude without stimulation. The startle response was measured for 100 ms from the startle pulse presentation, and the average value was defined as the startle amplitude. The startle amplitudes in response to repetitions of each trial type were averaged over the session. The test schedule was controlled by a microcomputer.

The percent prepulse inhibition (% PPI) of a startle response was calculated by the following formula:

$$\%\text{PPI at PP80} = \left\{1 - \frac{\text{PP80 \&P}}{\text{P alone}}\right\} \times 100$$

$$\%\text{PPI at PP70} = \left\{1 - \frac{\text{PP70 \&P}}{\text{P alone}}\right\} \times 100$$

2.8. Water-maze task training for spatial reference memory

We used the Morris water-maze task to test for an acquisition of spatial reference memory. The apparatus used for the hidden platform task in water-maze consisted of a white circular pool (diameter, 1.5 m; height, 0.5 m) filled to a depth of 20 cm with clear water (24±2 °C) and a transparent plastic platform (diameter, 15 cm; height, 0.3 m) submerged 2 cm below the water surface. Rats were given 6 consecutive training trials (a session) per day with an inter-trial interval of 60 s, from random starting location, with a hidden platform in a fixed position. Training sessions were performed over 5 consecutive days (total 30 trials). For each trial, rats had a maximum of 60 s swim time to mount the platform and they were then allowed to rest on the platform for additional 15 s. Rats were placed on the platform for 15 s manually if they elapsed. Rat position was tracked by computer, and the swim time was measured as the escape latency some rats that stayed longer making circle along the periphery of the pool in the session 1 were eliminated from the further training sessions.

On the last day of training session, a spatial probe test was conducted 60 s after the end of the last training session. Rats were given a 60 s-probe trial in which the hidden platform had been removed from the pool. For each probe test rat position was tracked by computer and the time spent in each quadrant zone was measured as the place preference. Each quadrant zone was defined as follows: target, the quadrant in which the hidden platform had been positioned; opposite, the quadrant opposite to the target; right, the quadrant on the right side of the target; left, the quadrant on the left side of the target.

2.9. Statistics

All statistical analysis was carried out by one-way ANOVA. Post–hoc individual comparison of paired groups was carried out by using Fisher's PLSD or the Student's *t*–test. A value of $P < 0.05$ was considered to represent a significant difference.

3. Results

3.1. Antisense-induced down-regulation of drebrin A protein levels and its time course

We first used Western blot analysis with antibodies against drebrin A and β-actin to examine the regional differences in the levels of drebrin A protein expression in the forebrain and cerebellum. Fig. 1 shows representative blots and quantitation of relative band densities for drebrin A and β-actin obtained from the neocortex, cerebellum, hippocampus, and thalamus of non-treated control rats. As shown in Fig. 1, drebrin A protein expression was clearly rich in the neocortex, hippocampus, and thalamus but poor in the cerebellum, while β-actin protein levels were almost uniform in all four brain regions.

We then examined the antisense-induced change in the protein levels in the two drebrin-rich regions of the forebrain, the neocortex, and hippocampus, at 4, 8, and 18 days after the intra-ventricular injection of HVJ-liposome vectors containing Dre-AS or Dre-RE. The levels of drebrin A protein in the neocortex of the rats treated with Dre-AS decreased markedly at 4 days after injection, remained reduced for several days, and returned to the original level by 18 days post-injection, while the levels of drebrin A protein in the Dre-RE-treated rats remained unchanged at 4 days post-injection. On the other hand, in the neocortex of the Dre-AS-treated rats and Dre-RE-treated rats, the β-actin protein levels did not change at any time post-injection (Fig. 2A). As shown in the quantitative analysis for drebrin A protein levels (Fig. 2B), a significant reduction of 53.7 ± 13.2% (mean ± S.E.M., $n = 7$, 4 days post-injection) or 44.7±12.1% (mean±S.E.M., $n = 7$, 8 days post-injection) in drebrin A protein level was specifically found in the neocortex of the Dre-AS-treated rats and was sustained for more than a week, while the Dre-RE treatment did not affect the drebrin A protein levels. As shown in the quantitative analysis for β-actin protein levels (Fig. 2C), a significant change of the β-actin protein levels was not found in the neocortex of the rats treated with Dre-AS or Dre-RE at any time post-injection.

The amount of drebrin A in the hippocampus of the rats treated with Dre-AS decreased markedly at 4 days after

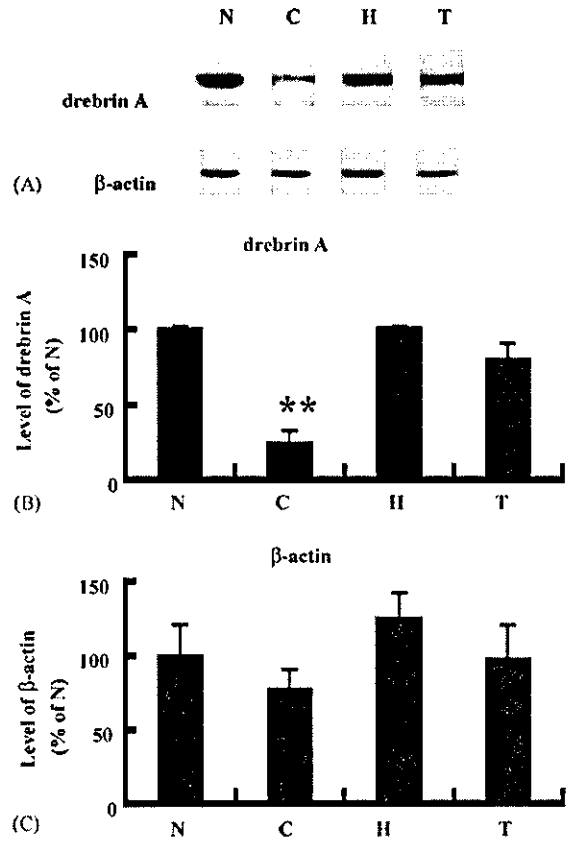

Fig. 1. Regional difference in the level of drebrin A protein expression in the brain of non-treated control rat. (A), Representative blots for drebrin A and β-actin obtained from the neocortex (N), cerebellum (C), hippocampus (H) and thalamus (T). Four μl of the homogenate (40 μg protein per lane) was loaded on 8% SDS gel for separation by electrophoresis. For measurement of β-actin as control protein, the membrane used for drebrin A was reprobed with monoclonal antibody against β-actin to confirm equal protein loading in each lane. (B–C) Quantitative analysis of relative band densities for drebrin A protein (B) and that for β-actin protein (C) obtained from the four brain structures. Level of drebrin A and β-actin protein in the four brain structures was represented as a percentage of that in the neocortex (N). Each value is an average of relative abundance of drebrin A protein or β-actin protein obtained from four non-treated rats ($n = 4$, mean ± S.E.M.). **Significantly different from the other three forebrain structures ($P < 0.01$).

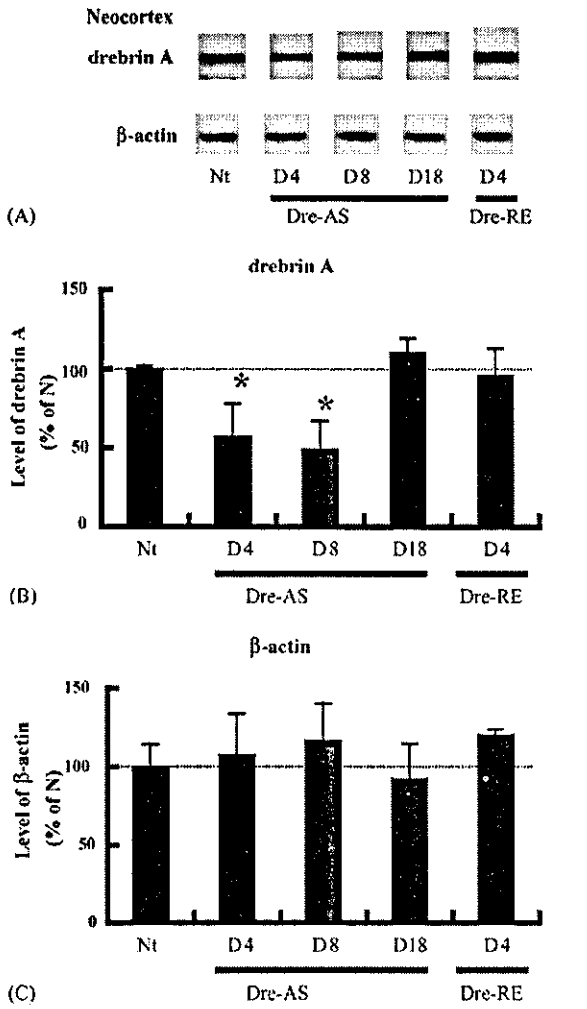

Fig. 2. Antisense-induced down-regulation of drebrin A protein expression in the neocortex and its time course following a single intra-ventricular injection of antisense ODNs to drebrin A by using HVJ-liposome mediated gene transfer method. Each treatment group: Nt, non-treated control rats; Dre-AS, rats that received an intra-ventricular injection of HVJ-liposome vectors containing antisense ODNs to drebrin A; Dre-RE, rats that received an intra-ventricular injection of HVJ-liposome vectors containing reversed antisense ODNs to drebrin A. (A) Representative blots for drebrin A and β-actin obtained from the neocortex of rats in each treatment group at 4 days (D4), 8 days (D8) or 18 days (D18) after an intra-ventricular injection of HVJ-liposome vectors containing ODNs. (B–C) Quantitative analysis of relative band densities for drebrin A protein (B) and β-actin protein (C) from the neocortex of rats in each treatment group. The relative density of each band was expressed as a percentage of the averaged density of bands in the Nt. Each value is an average of relative abundance of drebrin A or β-actin protein obtained from seven rats in each treatment group ($n = 7$, mean ± S.E.M.). *Significantly different from the Dre-RE (D4) ($P < 0.05$), and from the Nt and Dre-AS (D18) ($P < 0.01$).

injection, remained reduced for several days, and returned to the original level by 18 days post-injection, while the drebrin A protein levels in the Dre-RE-treated rats remained unchanged at 4 days post-injection. On the other hand, in the hippocampus of the Dre-AS-treated rats and Dre-RE-treated rats, the β-actin protein levels did not change at any time post-injection (Fig. 3A). As shown in the quantitative analysis for drebrin A protein levels (Fig. 3B), a significant reduction of 40.5 ± 8.9% (mean ± S.E.M., $n = 7$, 4 days post-injection) or 28.7 ± 11.8% (mean ± S.E.M., $n = 7$, 8 days post-injection) in drebrin A protein was specifically found in the hippocampus of the Dre-AS-treated rats and was sustained for more than a week, while the Dre-RE treatment did not affect the drebrin A protein levels. As shown in the quantitative analysis for β-actin protein levels (Fig. 3C), no significant change of the β-actin protein levels was found in the hippocampus of rats treated with Dre-AS or Dre-RE at any time post-injection.

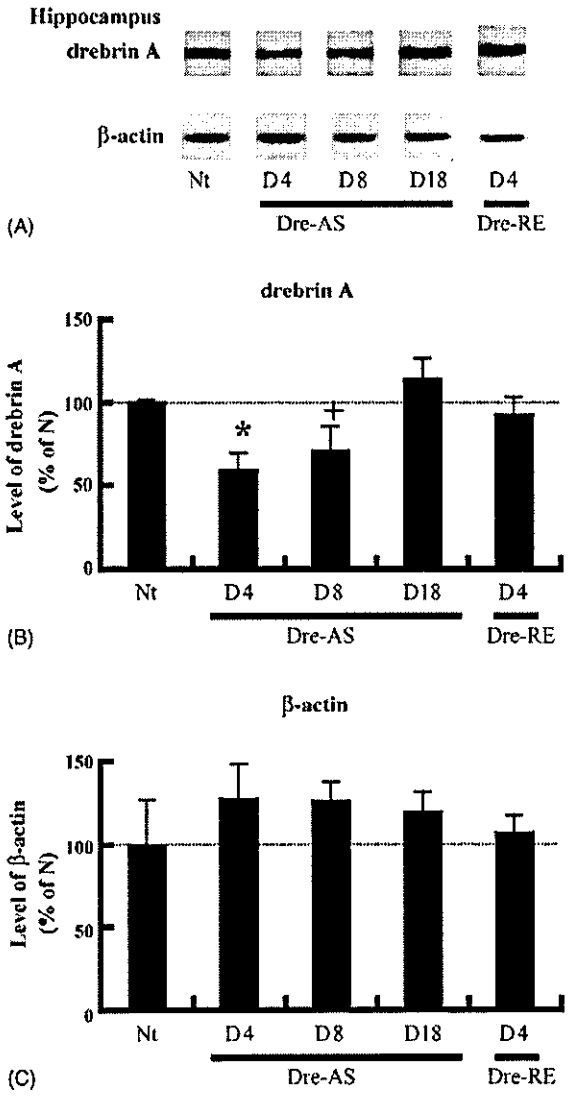

Fig. 3. Antisense-induced down-regulation of drebrin A protein expression in the hippocampus and its time course following a single intra-ventricular injection of antisense ODNs to drebrin A by using HVJ-liposome mediated gene transfer method. Each treatment group: Nt, non-treated control rats; Dre-AS, rats that received an intra-ventricular injection of HVJ-liposome vectors containing antisense ODNs to drebrin A; Dre-RE, rats that received an intra-ventricular injection of HVJ-liposome vectors containing reversed antisense ODNs to drebrin A. (A) Representative blots for drebrin A and β-actin obtained from the hippocampus of rats in each treatment group at 4 days (D4), 8 days (D8) or 18 days (D18) after an intra-ventricular injection of HVJ-liposome vectors containing ODNs. (B–C) Quantitative analysis of relative band densities for drebrin A protein (B) and β-actin protein (C) from the hippocampus of rats in each treatment group. The relative density of each band was expressed as a percentage of the averaged density of bands in the Nt. Each value is an average of relative abundance of drebrin A or β-actin protein obtained from seven rats in each treatment group ($n = 7$, mean ± S.E.M.). (+) Significantly different from the Nt ($P < 0.05$), and from the Dre-AS (D18) ($P < 0.01$). *Significantly different from the Dre-RE(D4) ($P < 0.05$), and from the Nt and Dre-AS (D18) ($P < 0.01$).

3.2. Increased spontaneous locomotion and abnormal adaptive behaviors in response to a novel environment in rats with drebrin A in vivo knockdown

To investigate the effects of antisense in vivo knockdown of drebrin A expression on adaptive behaviors in response to a novel environment, we recorded spontaneous locomotion and typical adaptive behaviors during a 30 min period in an open field test in rats that had received an intra-ventricular injection of HVJ-liposome vectors containing Dre-AS or Dre-RE 4 days prior to the open field test. The spontaneous locomotor activity was estimated by measuring the distance of locomotion during every 5 min period in the open field test of 30 min. On the other hand, the degree of typical adaptive behaviors, such as being exploratory, being stationary, or grooming in an open field, was estimated by measuring the total duration of being exploratory, being stationary, or grooming during the 30 min test period, respectively. The inserted figure in Fig. 4A shows the locomotor activity estimated by the total distance of spontaneous locomotion during the 30 min test period. As shown in the inserted figure, the locomotor activity in the Dre-AS-treated rats ($n = 9$) was significantly higher than that in the control Dre-RE-treated rats ($n = 6$). The time course of locomotor activity during the 30 min test period indicates that the significant increase of locomotor activity in the Dre-AS-treated rats is seen only in the earliest 5 min period during the 30 min open field test (Fig. 4A). As shown in Fig. 4B, the Dre-AS-treated rats ($n = 6$) were significantly less stationary and exhibited more grooming than the control Dre-RE-treated rats ($n = 5$).

3.3. Alterations in amphetamine-induced locomotor response in rats with drebrin A in vivo knockdown

To test whether abnormality of dopamine-related cortical functioning, which is believed to underlie some mental illnesses, is involved in behavioral alterations by the drebrin in vivo knockdown, we assessed the sensitivity to psychostimulant of the Dre-AS-treated rats using amphetamine-induced locomotor response. We measured locomotor activity in an open field during the 30 min period before amphetamine-injection (pre-injection phase) and the 60 min period after amphetamine-injection (post-injection phase) in rats that had received an intra-ventricular administration of HVJ-liposome vectors containing Dre-AS or Dre-RE 4 days prior to the amphetamine-induced locomotion test. The locomotor activity was estimated by measuring the locomotion during every 5 min period obtained from the total 90 min recording of locomotion in the open field. As shown in the post-injection phase in Fig. 5, a marked increase of the amphetamine-induced locomotor response was observed in the Dre-AS-treated rats. This increase by the Dre-AS treatment suggests that the Dre-AS-treated rats exhibit enhancement in the sensitivity to psychostimulant, compared with the sensitivity of the control Dre-RE-treated rats. It is notable that the degree of this increase of the

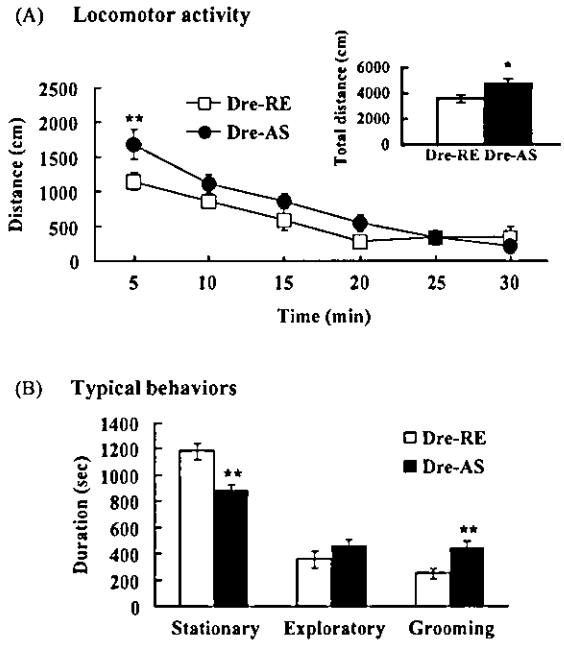

Fig. 4. Behavioral abnormalities in an open field test observed in rats with antisense in vivo knockdown of drebrin A expression. Treatment groups were: Dre-AS, rats that received a single intra-ventricular injection of HVJ-liposome vectors containing antisense ODNs to drebrin A 4 days prior to the open field test; Dre-RE, rats that received a single intra-ventricular injection of HVJ-liposome vectors containing reversed antisense ODNs to drebrinA 4 days prior to the open field test. The Dre-RE group was used as a control for the Dre-AS. (A) Increased locomotor activity in the Dre-AS rats during the open field test. Time-dependent change of spontaneous locomotor activity was estimated by locomotor distance during every 5 min following the start of locomotion in the open field. The inserted figure indicates the total locomotor distance during the 30 min test period. (B) Abnormal behavioral manifestations observed in the Dre-AS rats. Three typical behaviors that are characteristic of adaptive response to a novel environment: being stationary, being exploratory and grooming. Total duration of each behavioral manifestation was measured from the 30 min recording of behaviors in the open field by a chronometer, respectively. Each value represents mean ± S.E.M. ($n = 5$). *Significantly different from the Dre-RE ($P < 0.05$). **Significantly different from the Dre-RE ($P < 0.01$).

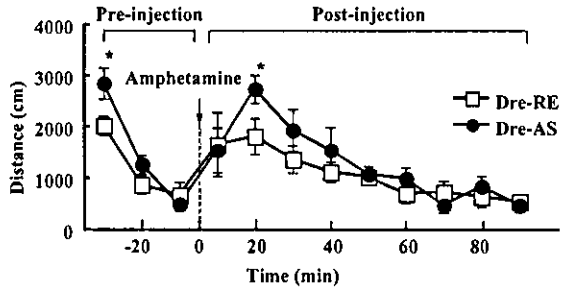

Fig. 5. Increased sensitivity to psychostimulant in an amphetamine-induced locomotor response observed in rats with antisense in vivo knockdown of drebrin A expression. Time-dependent change of locomotor activity before and after the intra-peritoneal injection of amphetamine was estimated by locomotor distance for every 5 min during the 30 min pre-injection and 60 min post-injection period. Treatment groups were: Dre-AS, rats that received a single intra-ventricular injection of HVJ-liposome vectors containing antisense ODNs to drebrin A 4 days prior to the amphetamine-induced locomotion test; Dre-RE, rats that received a single intra-ventricular injection of HVJ-liposome vectors containing reversed antisense ODNs to drebrinA 4 days prior to the amphetamine-induced locomotion test. The Dre-RE group was used as a control for the Dre-AS. Each value represents mean ± S.E.M. ($n = 6$). *Significantly different from the Dre-RE ($P < 0.05$).

amphetamine-induced locomotor response by the Dre-AS treatment and its recovery process are quite similar to that of the antisense-induced increase of the spontaneous locomotion in response to a novel environment, which is shown in the pre-injection phase in Fig. 5.

3.4. Reduction of pre-pulse inhibition and its recovery in rats with drebrin A in vivo knockdown

To examine whether the drebrin A in vivo knockdown causes a defect in the cognitive function, we used a PPI test of acoustic startle response. The PPI test was performed 4 and 18 days after the Dre-AS or Dre-RE treatment. The averaged startle amplitudes are shown in Table 1. The results from the PPI test performed 4 days after the treatment showed a significant disruption of PPI upon stimulation at PP70 but no significant disturbance of PPI at PP80 even

Table 1
Acoustic startle amplitudes in three types of stimulus trial and baseline amplitude in non-stimulus trial

Experiment	Treatment	Amplitudes in stimulus trial			
		B alone	P alone	PP70	PP80
Day 4	Dre-RE	5.2 ± 0.2	101.1 ± 15.1	40.5 ± 7.2	16.4 ± 1.7
	Dre-AS	4.7 ± 0.2	117.1 ± 20.9	71.0 ± 15.8	25.2 ± 4.9
Day 18	Dre-RE	5.0 ± 0.1	114.9 ± 23.9	46.2 ± 5.2	29.7 ± 7.2
	Dre-AS	6.3 ± 0.4	96.6 ± 4.2	45.0 ± 5.2	21.0 ± 1.5

Type of stimulus trial: B alone, non-stimulus trial to check the baseline amplitude without stimulation; P alone, stimulus trial with startle pulse alone; PP70, stimulus trial with the combination of startle pulse and 70 dB prepulse; PP80, stimulus trial with the combination of startle pulse and 80 dB prepulse. Experiment: Day 4, PPI test performed 4 days after the treatment with Dre-RE or Dre-AS; Day 18, PPI test performed 18 days after the treatment with Dre-RE or Dre-AS. Treatment group: Dre-RE, rats with intra-ventricular injection of reversed antisense ODNs to drebrin (Dre-RE); Dre-AS, rats with intra-ventricular injection of antisense ODNs to drebrin (Dre-AS). Each value represents mean ± S.E.M. ($n = 9$ for Day 4, $n = 6$ for Day 18).

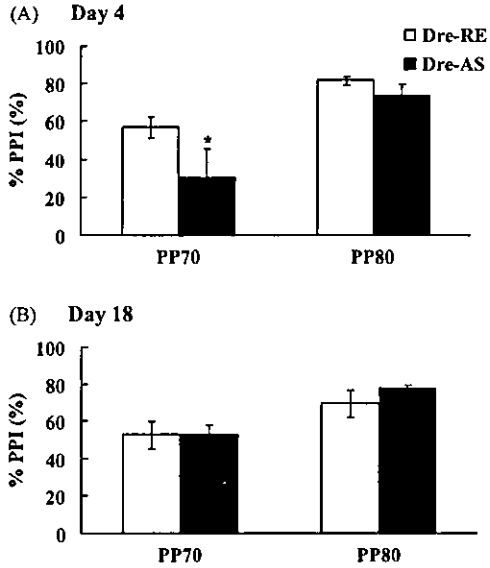

Fig. 6. Deficit of PPI of acoustic startle response and its recovery observed in rats with antisense in vivo knockdown of drebrin A expression. Treatment groups were: Dre-AS, rats that received a single intra-ventricular injection of HVJ-liposome vectors containing antisense ODNs to drebrin A 4 days or 18 days prior to the PPI test; Dre-RE, rats that received a single intra-ventricular injection of HVJ-liposome vectors containing reversed antisense ODNs to drebrinA 4 days or 18 days prior to the PPI test. The Dre-RE group was used as a control for the Dre-AS. The PPI was performed under two types of stimulation referred as PP70 and PP80. PP70 is an acoustic stimulation consisted of prepulse (20 ms burst of 70 dB) and startle-pulse (20 ms burst of 120 dB), while PP80 is that consisted of prepulse (20 ms burst of 80 dB) and startle-pulse (20 ms burst of 120 dB). (A) Percent prepulse inhibition in the Dre-AS or the Dre-RE 4 days after the ODNs-treatment. The rats treated with Dre-AS exhibited a significant disruption of PPI at the stimulation of PP70, but no disturbance of PPI at PP80 even though a slight tendency toward a reduced PPI. Each value represents mean ± S.E.M. ($n = 9$). *Significantly different from the Dre-RE ($P < 0.05$). (B) %PPI in the Dre-AS or the Dre-RE 18 days after the ODNs-treatment, when the down-regulated drebrin A expression has completely recovered to the original levels. The rats with Dre-AS treatment did not exhibit disruption of PPI at either PP70 or PP80, suggesting a recovery from the antisense-induced PPI deficit. Each value represents mean ± S.E.M. ($n = 6$).

though a slight tendency toward a reduced PPI was apparent compared with the control Dre-RE-treated rats (Fig. 6A). On the other hand, 18 days after the Dre-AS treatment, when the down-regulated drebrin A protein expression had completely recovered to the original levels, the Dre-AS-treated rats did not exhibit disruption of PPI at either PP70 or PP80 (Fig. 6B), suggesting a recovery from the antisense-induced PPI deficit.

3.5. Abnormality in the water-maze test in rats with drebrin A in vivo knockdown

To examine whether the antisense-induced down-regulation of drebrin A protein expression in the forebrain regions, such as the neocortex or hippocampus, causes an alteration in the acquisition of spatial reference memory, we used the Morris water-maze test. The rats received an intra-ventricular injection of HVJ-liposome vectors containing Dre-AS or Dre-RE 4 days prior to undergoing training in a water-maze. All of the rats in the treatment groups learned to swim directly to a hidden platform in five training sessions well before training was completed, as indicated in Fig. 7A. Compared with the rats treated with Dre-RE as a control group, a significant reduction in the escape latency was observed only in the earliest training session in the rats treated with Dre-AS.

On the last day of training, a spatial probe test was conducted just after the final training session. As shown in Fig. 7B, both Dre-AS-treated rats and control Dre-RE-treated rats spent more time in the target quadrant than in any other quadrant. However, surprisingly, the preference for the target quadrant observed in the Dre-AS-treated rats was significantly stronger than that in the control Dre-RE-treated rats, implicating that better spatial memory was acquired by the Dre-AS treatment.

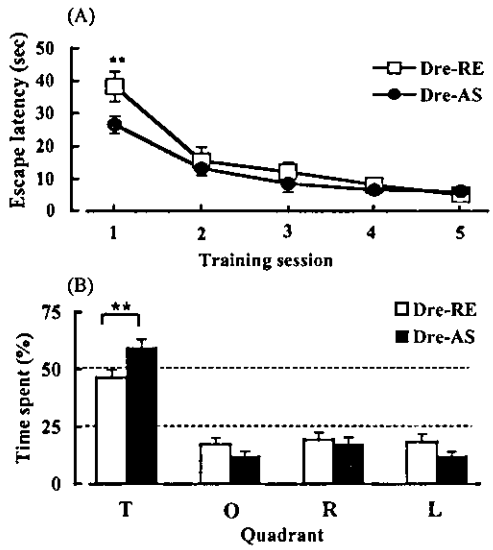

Fig. 7. Better memory in the hidden platform water-maze observed in rats with antisense in vivo knockdown of drebrin A. Treatment groups were: Dre-AS ($n = 9$), rats that received a single intra-ventricular injection of HVJ-liposome vectors containing antisense ODNs to drebrin A 4 days prior to the water-maze training; Dre-RE ($n = 6$), rats that received an intra-ventricular injection of HVJ-liposome vectors containing reversed antisense ODNs to drebrin A 4 days prior to the water-maze training. The Dre-RE group was used as a control for the Dre-AS. (A) Escape latency in water-maze training. Each value represents the averaged escape latency for 6 trials in each session (mean ± S.E.M.). The Dre-AS-treated rats displayed the greater learning ability during the first session in water-maze training than that of the Dre-RE. (B) Place preference in the spatial probe test conducted just after the end of training sessions. The Dre-AS-treated rats exhibited stronger preference for the target quadrant than that of the Dre-RE, suggesting that the Dre-AS-treated rats acquired better spatial memory. Quadrant was: T, target quadrant where the hidden platform was previously located; R, right quadrant; L, left quadrant; O, quadrant opposite to the target. **Significantly different from the Dre-RE ($P < 0.01$).

To clarify why the stronger preference for the target quadrant in Dre-AS-treated rats seems abnormal compared with that of non-treated control rats or Dre-RE-treated rats, we examined the time course of the place preference during 60 s probe trial. The upper panel of Fig. 8A shows a representative swimming track of a control Dre-RE-treated rat during the whole 60 s period of the probe test and its three divided tracks. The lower panel of Fig. 8A shows the place preference during every 20 s period following the start of the 60 s probe trial observed in control Dre-RE-treated

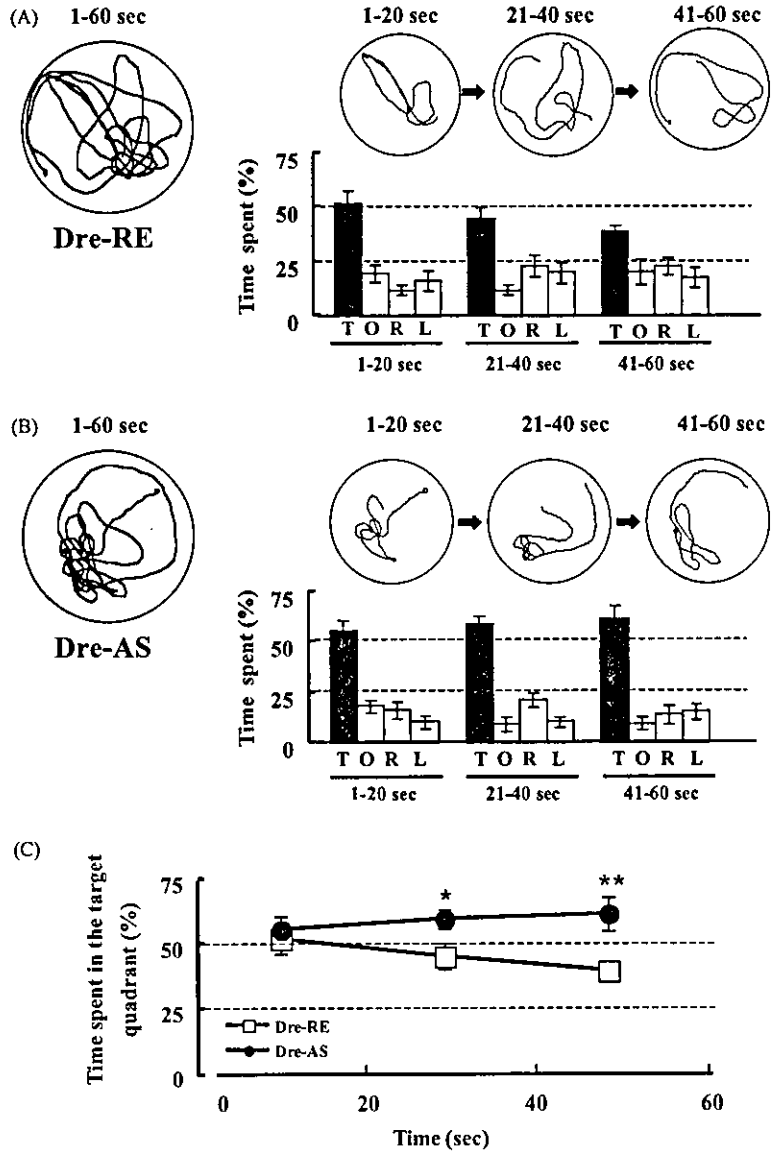

Fig. 8. Stronger preference for the target quadrant during the 60 s probe trial observed in rats with antisense in vivo knockdown of drebrin A. Treatment groups were: Dre-AS (n = 9), rats that received a single intra-ventricular injection of HVJ-liposome vectors containing antisense ODNs to drebrin A 4 days prior to the water-maze training; Dre-RE (n = 6), rats that received an intra-ventricular injection of HVJ-liposome vectors containing reversed antisense ODNs to drebrin A 4 days prior to the water-maze training. The Dre-RE group was used as a control for the Dre-AS. (A) Upper panel, representative swimming track of the control Dre-RE-treated rat during the 60 s period of the probe test and its three divided tracks; Lower panel, place preference during every 20 s period following the start of the 60 s probe trial observed in the Dre-RE-treated rats. The strong preference for the target quadrant in the Dre-RE rats declined within 60 s period of the probe trial. (B) Upper panel, representative swimming track of the Dre-AS-treated rat during the 60 s period of the probe test and those during every 20 s period following the start of a 60 s probe trial; Lower panel, place preference during every 20 s period following the start of the 60 s probe trial observed in the Dre-AS-treated rats. The strong preference for the target quadrant slightly increased within 60 s period of the probe trial. Unshadowed zone in the circle indicated the target quadrant, where the dense swimming track was depicted. (C) Time dependency of the strong preference for the target quadrant during 60 s period of the probe trial. In contrast to a decline in the strong preference for the target quadrant found in the Dre-RE-treated rats, the Dre-AS rats exhibited an abnormal persistence in the strong preference for the target quadrant. **Significantly different from the Dre-RE ($P < 0.01$). *Significantly different from the Dre-RE ($P < 0.05$).

rats (n = 9). As shown in the lower panel of Fig. 8A, the Dre-RE-treated rats as a control group exhibited a strong preference for the target quadrant zone in every 20 s period of the 60 s probe trial, but the level of preference for the target quadrant declined. This 60 s spatial probe test is originally designed to confirm an accomplishment of spatial learning by selection of a place preference in the water-maze without a hidden platform; that is, the same 60 s probe trial is not hypothesized to involve an additional behavioral response to the disappearance of the hidden platform task, which constitutes a problem that involves matching to sample. However, the decline in the preference for the target quadrant within the 60 s test period observed in the control rats suggests that behaviors in the 60 s spatial-probe test involve an adaptive response to a change of situation (namely, the disappearance of the hidden platform in the water-maze task), which is displayed by starting the searching behavior in quadrants other than the target quadrant in the water-maze. On the other hand, the upper panel of Fig. 8B shows a representative swimming track of the Dre-AS-treated rat during 60 s period of the probe test and its divided three tracks. The lower panel of Fig. 8B shows place preference during every 20 s period following the start of a 60 s probe observed in the Dre-AS-treated rats (n = 9). As shown in lower panel of Fig. 8B, the Dre-AS-treated rats exhibited a strong preference for the target quadrant in every 20 s period of the 60 s probe trial, and their preference for the target quadrant was sustained at the same level or slightly increased. As indicated in Fig. 8C, in contrast to the rapid decline that the control Dre-RE-treated rats exhibited in the preference for the target quadrant, the Dre-AS-treated rats displayed a rather slight increase in the level of their preference for the target quadrant within the 60 s probe trial. Thus, this abnormal persistence in the strong preference for the target quadrant zone in 60 s probe trial (Fig. 8C) suggests that the better spatial memory of the Dre-AS rats observed in Fig. 7B results from a cognitive deficit or worse judgment, which is revealed in their inability to inhibit inappropriate response to novel environment (namely, the disappearance of the hidden platform in the water-maze task).

4. Discussion

4.1. Antisense in vivo knockdown of drebrin A expression

We describe here the development of a rat with antisense-induced down-regulation of drebrin A protein levels in the drebrin-rich forebrain regions, such as the neocortex or hippocampus. The down-regulation of drebrin A protein levels that expressed 45–55% in the neocortex and 30–40% in the hippocampus was sustained for more than a week. The blocking effect of this intra-ventricular injection of antisense ODNs by using the HVJ-liposome method on the biosynthesis of drebrin A protein and the long-lasting action of antisense ODNs are equal to those of a repeated application or chronic infusion of antisense ODNs to NMDA-NR1 (Zapata et al., 1997). In a previous study, it was demonstrated that the Dre-AS we used here prevented the biosynthesis of drebrin A protein by about 48% in cultured cortical neurons (Takahashi et al., 2003; Tanaka et al., 2001). The present rate (45–55% in the cortex and 30–40% in the hippocampus) of an in vivo knockdown of drebrin A induced by the intra-ventricular administration of HVJ-liposome vectors containing Dre-AS was consistent with the rate of the in vitro knockdown of drebrin A induced by De-AS. In addition, since the transfection efficiency in vivo of HVJ-liposomes containing a plasmid DNA of constitutive nitric oxide synthase (c-NOS) has been reported to be 40–50% (Kaneda, 1999), the rate of an antisense in vivo knockdown of drebrin A by using HVJ-liposome vectors suggests that the biosynthesis of drebrin A in the transfected neurons is almost completely prevented by the long-lasting action of antisense ODNs, which are introduced into neurons bypassing the lysosomal attack. Thus, the degree of in vivo knockdown of drebrin A by a single intra-ventricular infusion of HVJ-liposome containing Dre-AS and its long-lasting action are sufficient to allow behavioral analysis for investigating the role of some specific proteins in higher brain functions without the stressful implantation of a cannula for repetitive or chronic administration.

4.2. Behavioral alterations induced by a drebrin A in vivo knockdown

Drebrin A in vivo knockdown rats display increased locomotor activity, a decreased stationary state, and enhanced grooming as adaptive behaviors in an open field and marked increase in an amphetamine-induced locomotor response (see Figs. 4 and 5). It could be considered that the decreased stationary state simply reflects the increase of locomotor activity due to unchanged locomotor velocity. Both increased locomotor activity in the earliest session and enhanced grooming in the open field test are a typical anxiety-like behavior for rodents as an adaptive response to a novel environment. It is commonly believed that changes in dopaminergic tone are highly related to alterations in locomotor activity (Amara and Kuhar, 1993; Giros et al., 1996), which explains the amphetamine-induced locomotor response. Therefore, the increase in amphetamine-induced locomotor response in the Dre-AS knockown rats, indicating their hypersensitivity, is thought to be an outcome of the increased sensitivity to psychostimulant in the drebrin knockdown rats. In addition to alteration in an emotional state, such as anxiety, alterations in locomotor behavior due to an increased sensitivity to psychostimulant have also been correlated with a positive symptom of schizophrenia (Corbett et al., 1995; Malhotra et al., 1997). Thus, an antisense-induced in vivo knockdown of drebrin A expression results in a number of altered behaviors that have been